ROCK FORMATION CHARACTERIZATION FOR CARBON DIOXIDE GEOSEQUESTRATION: 3D SEISMIC AMPLITUDE AND COHERENCY ANOMALIES, AND SEISMIC PETROPHYSICAL FACIES CLASSIFICATION, WELLINGTON AND ANSON-BATES FIELDS, SUMNER COUNTY, KANSAS, USA

by

DEREK ROBERT OHL

B.A., Kansas State University, 2010

A THESIS

submitted in partial fulfillment of the requirements for the degree

MASTER OF SCIENCE

Department of Geology
College of Arts and Sciences

KANSAS STATE UNIVERSITY
Manhattan, Kansas

2012

Approved by:

Major Professor
Dr. Abdelmoneam Raef

Copyright

Abstract

Amid increasing interest in geological sequestration of carbon dioxide (CO_2), detailed rock formation characterization has emerged as priority to ensure successful sequestration. Utilizing recent advances in the field of 3D seismic attributes analysis, offers improved opportunities to provide more details when characterizing reservoir formations. In this study, several post-stack seismic attributes integrated with seismic modeling for highlighting critical structural elements and petrophysical facies variation of rock formations at Wellington and Anson-Bates fields, Sumner County, Kansas. A newly acquired 3D Seismic data set and several geophysical well logs are also used to achieve the objectives of this study. Results sought in this study are potentially important for understanding pathways for CO_2 to migrate along.

Seismic amplitude, coherency, and most negative curvature attributes were used to characterize the subsurface for structural effects on the rock formations of interest. These attributes detect multiple anomaly features that can be interpreted as small throw faults. However, in this study, there is a larger anomalous feature associated with the Mississippian formation that can be interpreted as a small throw fault or incised channel sand. Determining which of the two is very important for flow simulation models to be more exact.

Modeling of the seismic was undertaken to help in the interpretation of the Mississippian amplitude anomaly. An artificial neural network, based on well log porosity cross-plots and three seismic attributes, was trained and implemented to yield a seismic petrophysical facies map. The neural network was trained using three volume seismic waveform attributes along with three wells with difference in well log porosity. A reworked lithofacies along small throw

faults has been revealed based on comparing the seismic structural attributes and the seismic petrophysical facies.

Arbuckle formation characterization was successful to a certain degree. Structural attributes showed multiple faults in the northern half of the survey. These faults are in agreement with known structure in the area associated with the Nemaha uplift. Further characterization of the Arbuckle was hindered by the lack of well data.

This study emphasizes the need for greater attention to small-scale features when embarking upon characterization of a reservoir for CO_2 based geosequestration.

Table of Contents

List of Figures vi
Acknowledgements xi
Chapter 1 - Introduction 1
Summary 1
Significance 2
Literature Review 4
Study Area 6
Production Data and Field History 8
Geologic CO_2 Sequestration 10
Chapter 2 - Geologic Setting and Stratigraphy 13
Structure 13
Stratigraphy 15
Chapter 3 - Data Acquisition and Methods 22
3D Data Acquisition 22
Interpretation Methods 26
Synthetic Seismic Modeling 26
Horizon Tracking 30
Seismic Attributes 32
Amplitude 32
Coherency 34
Curvature 35
Seismic Petrophysical Facies Modeling 37
Chapter 4 - Results and Discussion 41
Mississippian Characterization 41
Arbuckle Characterization 62
Chapter 5 - Conclusion 72
References 74

List of Figures

Figure 1 Displays a map of the state of Kansas with electric producing power plants in blue and red boxes (top nine CO_2 producers are in red). The grey areas in the back ground represent known producing oil fields. (Figure from www.kgs.ku.edu/CO2/resource/index.html)..... 4

Figure 2 Shows the outlines of the two 3D seismic data sets merged together in order to form one large study area. The green outline denotes the Wellington 3D seismic data while the blue outline represents the Anson-Bates 3D seismic data purchased from Nobel Energy. (Map from KGS) 7

Figure 3a, on the left, shows the location of the State of Kansas (shaded) in respect to the United States of America. Figure 3.b on the right, shows the location of Sumner County (Red Star) in regards to the state of Kansas. (Pictures from www.bankofamerica.com & www.kansasnativeplantsociety .org) 7

Figure 4 Shows a map of Sumner County, Kansas with the Wellington oil field depicted by the red star. (Picture from the KGS) 8

Figure 5 Shows the major producing oil fields located within the 3D seismic coverage. Also displayed are the oil fields cumulative production values in barrels (bbls). (Picture modified from the KGS)..... 10

Figure 6 Cartoon showing multiple ways of storing carbon dioxide in geologic formations (Bachu 2003). 12

Figure 7 Map of Kansas showing major structural features. 13

Figure 8 Shows inferred Precambrian basement structures throughout Kansas. The red star is the location of the study area while the red lines are faults associated with the Nemaha uplift. (http://www.kgs.ku.edu/Publications/Bulletins/233/Baars/) 14

Figure 9 General stratigraphic column of the state of Kansas showing the main formations of study highlighted in yellow (Carr et al 2005). 17

Figure 10 Geophysical well logs (GR-gamma ray, SP-spontaneous potential, CAL-Caliper, PE-photoelectric, NPHI- neutron porosity, RHOB-density, DPHI-density porosity) showing multiple sealing formations above the Mississippian formation. Red boxes show shale members that are potential sealing formations. 18

Figure 11 Geophysical well logs (same logs as in Figure 10) showing multiple sealing formations present. Red boxes show shale members that are potential sealing formations. Yellow boxes show formations being considered for geologic sequestration of carbon dioxide..... 19
Figure 12 West to east cross-section of southern Kansas showing major stratigraphic units and their general behavior as you move from the Hugoton Embayment in western Kansas to the Cherokee basin in southeastern Kansas. Red box and red star signify the location of the study area. (http://www.kgs.ku.edu/Publications/Bulletins/162/03_strat.html#Fig5)..... 21
Figure 13 Shows the Paragon Geophysical Services recording station. Figure 14 Shows the single 3C Digital geophone planted in the ground ready for listening. 23
Figure 15 Shows the two vibroseis sources used to acquire the seismic data. 24
Figure 16 Showing the outlines of the two 3D seismic surveys. Green is the outline of the Wellington 3D and the blue outline is for the Anson-Bates 3D survey. (Picture modified from the KGS)..... 25
Figure 17 Raw synthetic seismogram for the Wellington KGS 1-28 well. 28
Figure 18 Edited synthetic seismogram for the Wellington KGS 1-28 well. 29
Figure 19 Seismic amplitude section with tracked time horizons (depicted by the red (Heebner), green (Kansas City), blue (Mississippian), purple (Arbuckle), and yellow (Basement) lines) corresponding to those formation tops. (Ohl and Raef, 2012. Journal of Applied Geophysics, under review)..... 31
Figure 20 Coherency attribute comparing multiple seismic traces around a single trace. (Chopra and Marfurt, 2007)..... 35
Figure 21 Diagram showing 2D curvature along a reflector; positive curvature is associated with anticline features, negative curvature is associated with a flat surface or dipping plane, and zero curvature is associated with syncline features (modified from Roberts 2001). 36
Figure 22 Schematic demonstrating the process of neural network correlation between input layers and hidden layers to produce an output layer. In the case of this study, waveform attributes were the input layer while well log porosity classes were the hidden layer to produce the petrophysical facies map. (psycnet.apa.org)..... 38
Figure 23 Average Mississippian porosities and seismic horizon amplitude for the Mississippian top. Seismic amplitudes show some correlation with Mississippian porosity. 40

Figure 24 Mississippian horizon showing seismic amplitude variation. A large anomalous feature is seen trending NNW-SSW and is pointed out by arrows. 42
Figure 25 Shows the signal to noise spectrum extracted from the anomalous area. 43
Figure 26 Shows the extracted signal to noise spectrum for the entire survey. It is important to note the similarity between the two spectrums and as a result the anomaly is not an artifact. 43
Figure 27 (a) Seismic amplitude extracted along the horizon of the Mississippian-top in the Wellington 3D seismic data set with locations of seismic cross sections shown in (b), (c) and (d) with amplitude dimming (marked with ellipses). (Ohl and Raef, 2012. Journal of Applied Geophysics, under review) 45
Figure 28 Coherency attribute Mississippian horizon map showing the linear anomaly trending NNE. The green arrows denote the fault/fracture orientation within the study area which correlates very well with features caused by the Nemaha Uplift as seen back in Fig. 1b; the yellow circle shows the location of a proposed CO2 injection site and the green arrows to coherency anomalies K through to N. (Ohl and Raef, 2012. Journal of Applied Geophysics, under review) 47
Figure 29 Most negative curvature map generated in house showing fault and fracture patterns within the seismic survey. Red areas show possible faults within the seismic survey. 49
Figure 30 Most negative curvature for the study area calculated by Susan Nissen at Geotexture. 50
Figure 31 Showing the Mississippian porosity values for wells throughout the survey broken into their respected petrophysical facies classes to be used in the neural network. 52
Figure 32 Class-type wells in the selected attributes cross-plot space that was used to train the neural network. (Ohl and Raef, 2012. Journal of Applied Geophysics, under review) 53
Figure 33 Performance test in mean squared error with iterations “epochs” of the training, validation, and applied LVQ network. (Ohl and Raef, 2012. Journal of Applied Geophysics, under review) 54
Figure 34 Seismic (petrophysical/lithological) facies map of the Mississippian based on the application of the trained competitive neural network. (Ohl and Raef, 2012. Journal of Applied Geophysics, under review) 55

Figure 35 Seismic (petrophysical/lithological) facies map of the Mississippian with the coherency lineaments overlaid as dashed lines; the solid line indicate location of amplitude anomaly where it deviates from the corresponding lineament "N" of Figure 28. (Ohl and Raef, 2012. Journal of Applied Geophysics, under review) 56
Figure 36 Cross-plot of well log porosity against acoustic impedance of the Mississippian indicating separable clustering based on acoustic impedance, at three not-selected in training the ANN, wells, thus relevance of seismic wavelet characteristics (bandwidth, energy, and peakedness) to petrophysical facies classification for the Mississippian depleting reservoir. The wells used in this cross-plot were color coded so as to correspond to their petrophysical class color as seen in Figure 35. (Ohl and Raef, 2012. Journal of Applied Geophysics, under review)..... 57
Figure 37 Shows the OpendTect neural network petrophysical facies map for the top fifty feet of the Mississippian formation. High porosity values are seen in green, moderate porosity values are in blue, while low porosity values are yellow..... 59
Figure 38 Misclassification of the seismic data by the neural network. The misclassification was at, or below, five percent, resulting in a high quality correlation between the seismic data and the neural network. Test data is blue in color while train data is red in color. 60
Figure 39 Shows multiple wells for each petrophysical facies class falling within their respected classes giving further validation that the process was successful in its training and application of the neural network. 61
Figure 40 Arbuckle amplitude map demonstrating amplitude anomalies in the upper Arbuckle formation. Red arrows show possible faulting seen in the amplitude map. 63
Figure 41 Arbuckle coherency map showing faults in the Anson-Bates portion of the survey. Yellow arrows show very similar lineaments as seen in Figure 40. This lineaments are interpreted as faults. 65
Figure 42 Seismic cross-section showing interpreted faults (red lines) in the Anson-Bates survey that was donated by Nobel Energy. 66
Figure 43 Arbuckle curvature showing similar results as the coherency. Faulting is present in the Anson-Bates portion of the survey. Curvature also shows the fault and fracture pattern for the upper Portion of the Arbuckle formation. The trend of the fault and fracture pattern is in agreement with the Nemaha Uplift trend. 68

Figure 44 Average Arbuckle porosities for wells, which penetrate the Arbuckle formation far enough, that helped train the neural network to characterize the Arbuckle horizon in terms of petrophysical facies. 69
Figure 45 Petrophysical facies map of the Arbuckle horizon. High porosity values are seen in green, moderate porosity values are in blue, while low porosity values are yellow..... 70
Figure 46 Arbuckle neural network misclassification chart showing average misclassification of the Arbuckle horizon at 10 percent. Test data is blue in color while train data is red in color. 71

Acknowledgements

I would like to thank several people for their involvement in the completion of my Master's thesis. First off I would like to thank my major professor Dr. Abdelmoneam Raef for taking me on as his graduate student and also for the numerous occasions that I would interrupt him in his office to ask questions. I would also like to thank my other committee members Dr. Jack Oviatt and Dr. Matthew Totten for their guidance and support. I would like to thank the Department of Energy and the Kansas Geological Survey for sponsoring my research. I would like to thank IHS Kingdom for providing the Kingdom Suites software through their educational grant. To my fellow graduate students, I would like to say thank you for brainstorming sessions and the ever so often distraction. Last I would like to thank my wife, Ashley Ohl, for her continued support throughout my educational career.

Chapter 1 - Introduction

Summary

It is a known fact that carbon dioxide levels are on the rise in today's atmosphere. It is postulated that this rise in carbon dioxide levels is resulting in global warming conditions. Due to this concern it is important to help mitigate the levels that are released into the atmosphere. There are currently several options that can be applied simultaneously on how to mitigate carbon dioxide; 1) increase usage of clean renewable energy 2) decrease fossil fuel consumption 3) capture the carbon dioxide at point sources and dispose of it. All of the options are useful in mitigation, but of the three the last one is likely to be the most impactful in the near future.

This study focuses on the importance of characterizing subsurface rock formations for potential sequestration of carbon dioxide. In order to safely sequester carbon dioxide in the subsurface, a better overall understanding of this process is necessary. With enhancement of characterization techniques and minute feature details, the sequestration plume should be able to be more accurately modeled. This study is concerned with using the enhanced techniques within the geophysics community to better characterize the rock formations for carbon dioxide sequestration. Multiple 3D seismic attributes, geophysical well logs, and artificial neural networks give insight to potential pathways for the carbon dioxide to migrate along and provide petrophysical parameters for CO_2 flow simulation modeling.

This enhanced seismic characterization provides important rock formation details, such as but not limited to fault and fracture patterns, which would then be incorporated in a carbon dioxide plume model. Adding these key details to the subsurface rock formation model will give

more accurate results and potentially help geoscientists better understand, verify, and monitor carbon dioxide sequestration in rock formations.

Significance

The injection and storage of captured CO_2 in geological formations has been postulated as a strategy to significantly reduce overall CO_2 emissions into the atmosphere (Friedmann S.J., 2007; Sundquist et al., 2008; Bickle M.J., 2009). With fossil fuel consumptions increasing from year to year, a rise in the emissions of greenhouse gases are inevitable and needs to be dealt with accordingly. With carbon emissions on the rise and no real means to an end in sight, the main objective of this study is to increase knowledge about reservoir formation properties, such as porosity, permeability, faulting, fracturing, and possible channel fills, in order to build the most up to date flow simulation for CO_2 sequestration. Characterizing reservoir formations for CO_2 sequestration is more complex than characterizing for oil due to the complex properties of CO_2 in the supercritical state. More attention to building detailed subsurface rock formation models is essential in order to enable robust flow simulation. Miss-interpreting one little fault or channel could mean that the CO_2 plume would venture from the modeled path, which could lead to other unpredicted problems.

Rock formation characterizations can pose many challenges for geoscientists when tackling carbonate rocks, due to their notorious lithofacies heterogeneities at relatively high spatial frequency. In such rock characterization projects, it is a high risk to build flow simulation models based on sparse well data of low spatial coverage. In a carbonate case study of enhanced oil recovery using CO_2 in central Kansas (Raef et al. 2005), time lapse monitoring of CO_2 flood progression did not agree with initial flow simulation models. The flow simulation model was built honoring bulk lithological properties and wellhead pressure data. It is an essential

component of our current study during rock formation characterization, for CO_2 enhanced oil recovery and subsequent carbon geosequestration, to investigate amplitude and coherency attribute anomalies.

Figure 1, displays all active power plants within the State of Kansas as color filled boxes with the top ten CO_2 producing power plants illustrated by the red boxes. The smaller grey areas in the background display known oil and gas fields throughout the state of Kansas. These known fields are key factors in the potential sequestration of produced CO_2. A majority of the fields in the state of Kansas produce from the Kansas City, Mississippian, or Arbuckle formations. The Arbuckle formation will be discussed in further detail, but it is important to note that the Arbuckle is currently used as an oil field waste water disposal formation consisting of a large saline aquifer. The potential U.S. storage capacity of deep porous rock formations that contain saline ground water is approximately 900 to 3400 gigatons of carbon, (estimated by the Department of Energy) but less is known about the effectiveness of trapping mechanisms for these formations (Sundquist et al., 2008).

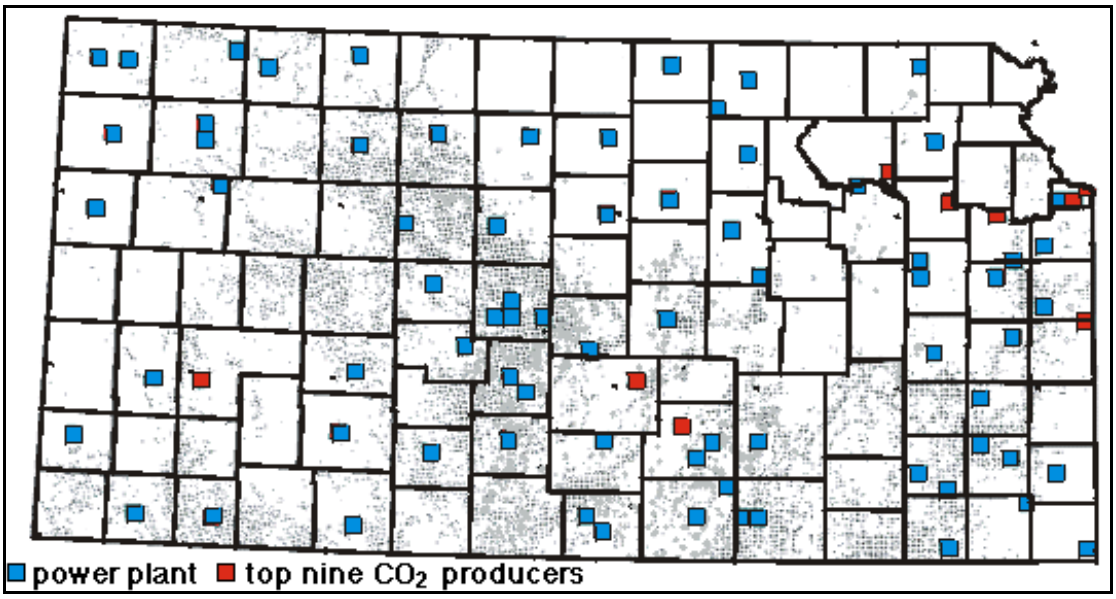

Figure 1 Displays a map of the state of Kansas with electric producing power plants in blue and red boxes (top nine CO_2 producers are in red). The grey areas in the back ground represent known producing oil fields. **(Figure from www.kgs.ku.edu/CO2/resource/index.html)**

Literature Review

Characterization of saline aquifers and depleting hydrocarbon reservoirs for carbon dioxide, geosequestration is an ongoing effort exemplified by several case studies around the world such as Sleipner field; North Sea (Torp and Gale 2004; Arts et al. 2004), Krechba; Algeria (Mathieson et al. 2009), and Ketzin; Germany (Kazemeini et al. 2009). These larger CO_2 case studies have paved the way for many smaller scale studies such as the Wellington Oil Field CO_2 project in south central Kansas.

Depleting hydrocarbon reservoirs are good candidates for tertiary enhanced oil recovery based on CO_2 sequestration, and subsequent carbon geosequestration (Litynski et al., 2008). It is noteworthy that the deeper less penetrated saline aquifer posed many more characterization challenges compared to the depleted hydrocarbon reservoir. In response to the need of high-resolution characterization, we are using post-stack seismic attributes, sonic well logs, and

artificial neural network training to assist in the characterization of Mississippian and Arbuckle carbonates.

The higher relative mobility of CO_2 in comparison to crude oil or brine highlights the need for higher resolution characterization when embarking upon carbon geosequestration projects, especially in carbonate rock formations. Candidate case studies of CO_2 based enhanced oil recovery (Damen et al. 2005; Doughty et al., 2008) or current case studies, e.g. Holtz et al. (2001) may justify focus upon possibilities of CO_2 flooding progression that can be either partially controlled by lithofacies, rather than reservoir pressure gradient, or can play as slip-inducing factor along minor or major faults. Due to multiple influences on CO_2 flood progression, we emphasize the need of higher resolution characterization than what would usually be sufficient for hydrocarbon production. Nevertheless, lessons learned and empirical relationships established and validated during CO_2 enhanced oil recovery could prove very beneficial in characterizing the far less studied saline aquifers. Especially when considering multi-target characterization, in the same sedimentary basin for large-scale carbon geosequestration projects.

Several reports suggest that saline aquifer formations are the best viable option for sequestering large amounts of CO_2. The global storage capacity in saline aquifers is estimated at several thousand gigatonnes or approximately around 50 to 100 years worth of emissions (Bickle, 2009). Kansas, Missouri, and Oklahoma comprise one of the largest regional-scale saline aquifer systems in North America (Carr et al., 2005). This large-scale saline aquifer system is known as the Ozark Plateau aquifer system. On the regional level, sequestration capacity in the Ozark Plateau aquifer system is enormous and the seal integrity is excellent (Carr

et al., 2005). Kansas' potential for CO_2 sequestration in saline aquifers is estimated at 18,078 million tones, according to the Department of Energy's 2010 Carbon Sequestration Atlas.

Study Area

The study area is located within a twenty square mile 3D seismic survey, of which twelve square miles were acquired by the Department of Energy to help better characterize rock formations for geologic carbon dioxide sequestration. Figure 2, shows the outline of the two 3D seismic data sets that were merged together to form the twenty square mile study area. The green outline denotes the Wellington 3D seismic data acquired by the Department of Energy in March and April of 2010, while the blue outline represents the Anson-Bates 3D seismic data purchased from Nobel Energy. The 3D seismic survey encompasses five significant oil fields with a total cumulative production of 27,569,074 barrels of oil since the 1960's.

The Wellington Oil field, which is the primary study area, is located in Sumner County Kansas. Sumner County is located in south central Kansas, as shown in Figure 3. Within Sumner County the Wellington Oil field is located in the north central part of the county, as seen in Figure 4, just a couple of miles to the northwest from the city of Wellington. The Wellington Oil Field was chosen as the primary study site, by the Department of Energy, for a couple of reasons: 1) it is a depleted hydrocarbon reservoir, 2) it has a lower formation that is part of a saline aquifer system, and 3) the over lying rock formations are believed to have excellent seal qualities.

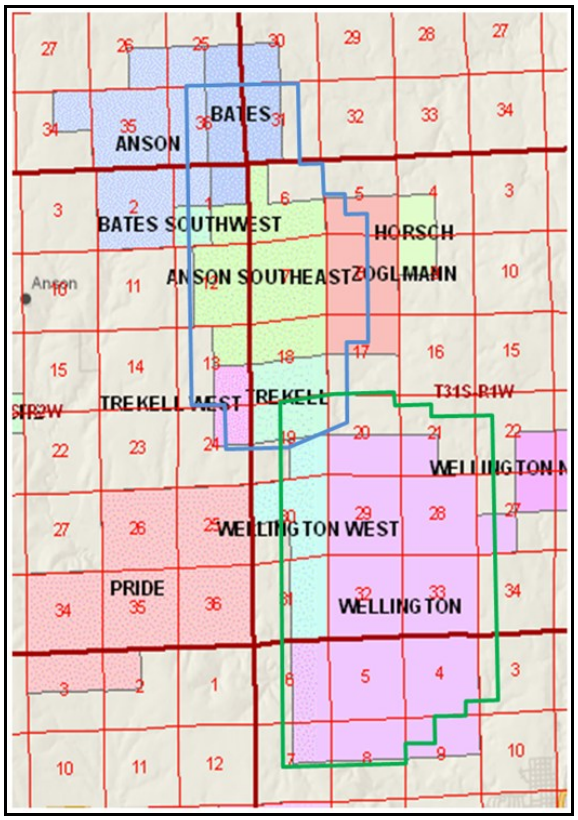

Figure 2 Shows the outlines of the two 3D seismic data sets merged together in order to form one large study area. The green outline denotes the Wellington 3D seismic data while the blue outline represents the Anson-Bates 3D seismic data purchased from Nobel Energy. **(Map from KGS)**

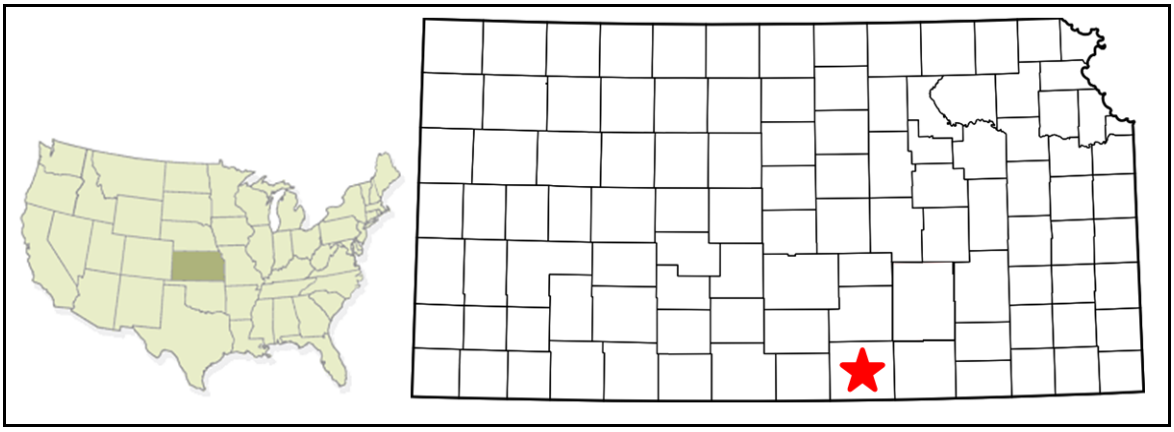

Figure 3a, on the left, shows the location of the State of Kansas (shaded) in respect to the United States of America. Figure 3.b on the right, shows the location of Sumner County (Red Star) in regards to the state of Kansas. **(Pictures from www.bankofamerica.com & www.kansasnativeplantsociety .org)**

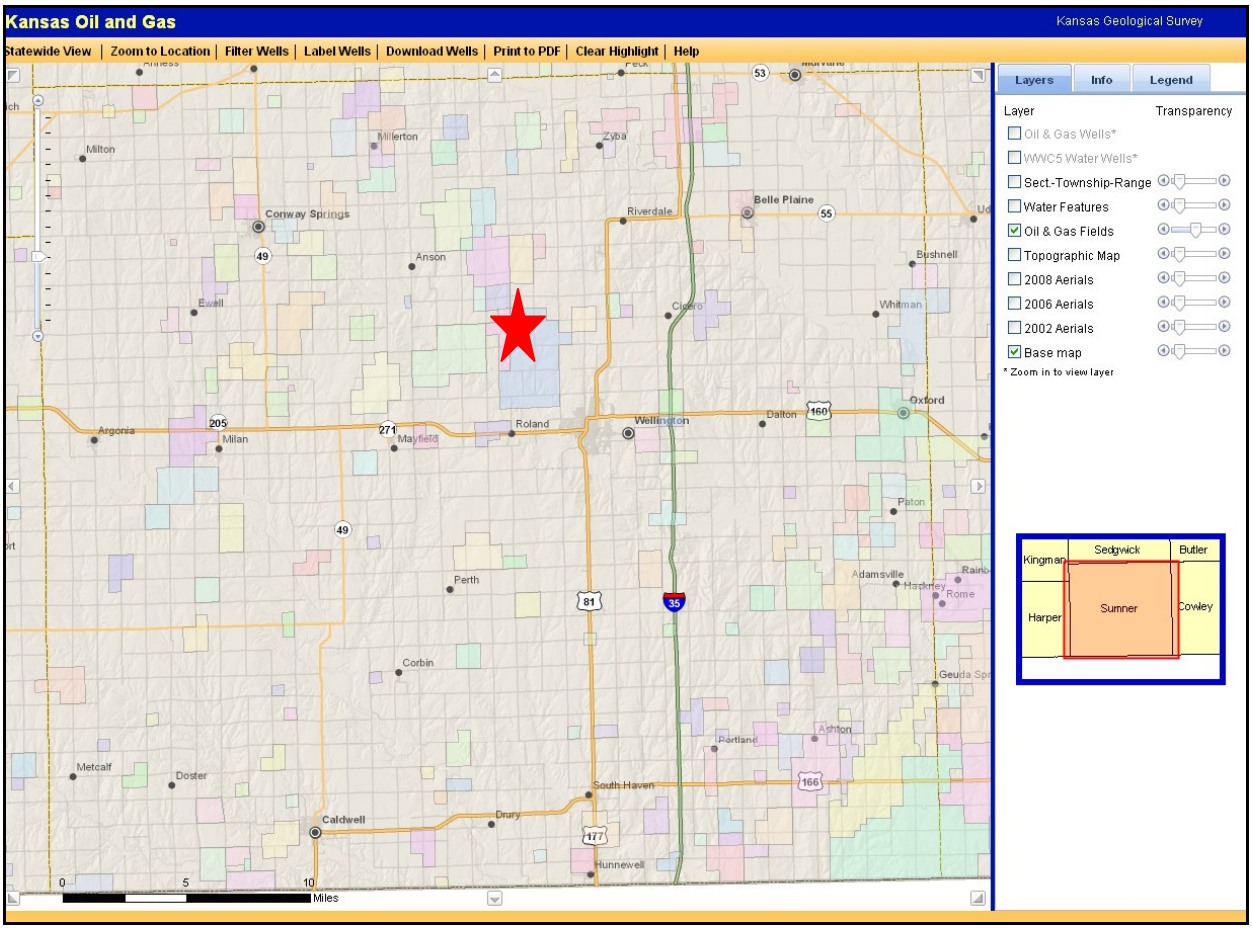

Figure 4 Shows a map of Sumner County, Kansas with the Wellington oil field depicted by the red star. (Picture from the KGS)

Production Data and Field History

The Wellington field, the primary field of study, was discovered in the late 1920's by an operator named Slick and Others. Production in the Wellington Field is primarily from the limestone of the Mississippian formation; later production from the Kansas City formation production was discovered. The cumulative production of oil from the Wellington Field as of last year, 2011, is 20,605,891 bbls. This volume of oil being produced from the Wellington Field encouraged other operators to expand north and west, discovering five other fields of significant oil production (Figure 5). The Anson South East field was discovered in the late

1950's by Beardmore Drilling, and has a cumulative production of 4,235,752 bbls of oil. The Trekell and Bates Fields were also discovered by Beardmore Drilling in the late 1950's and early 1960's. These two fields have a combined cumulative production of 1,922,795 bbls of oil since their discovery. In the 1970's Zenith Drilling expanded within the Wellington Field discovering the Wellington West Field which has a cumulative production of 736,816 bbls of oil to date. All of these fields primary production is from the Mississippian formation.

The average drop in hydrocarbon production for these five fields, within the study area, is 91.6%. It is important to bring to attention the fact that the majority of these fields have been involved with an active water flood since before the 1980's. This drastic drop in production over the years demonstrates the need for secondary enhanced oil recovery, potentially using CO_2 floods. Dyer and Farouq Ali (1991), state that the most important effect of carbon dioxide on the crude oil system is the large reduction in oil viscosity. This lowering of the oil's viscosity can help to achieve maximum recovery within a field during CO_2 sequestration, due to easier oil migration.

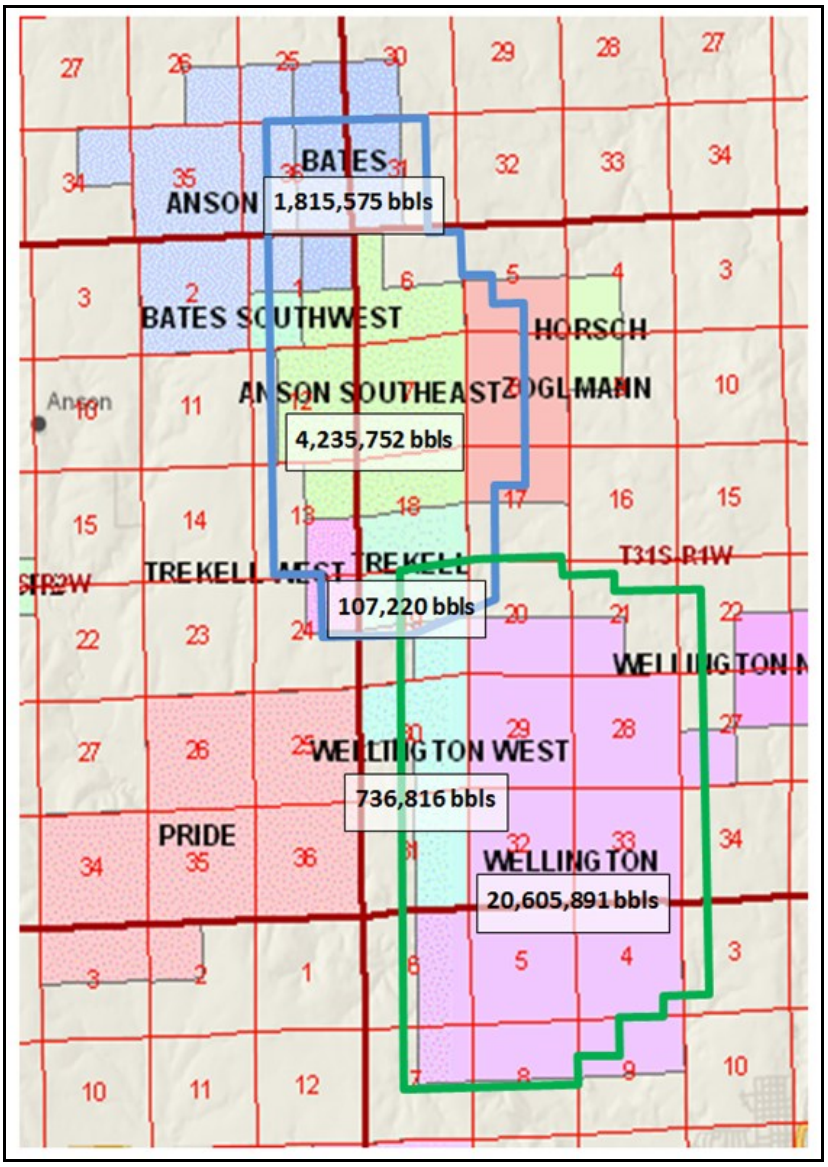

Figure 5 Shows the major producing oil fields located within the 3D seismic coverage. Also displayed are the oil fields cumulative production values in barrels (bbls). (Picture modified from the KGS)

Geologic CO_2 Sequestration

Geologic carbon dioxide sequestration is the process of mitigating carbon emissions by storing captured CO_2 in different geological mediums. Geologic sequestration of CO_2 is a more viable mitigation technique than the sequestration of CO_2 in the world's oceans, because of the

retention times of storage between the two mediums. Retention times for the world's oceans range from 10-10^5 years (Bachu 2003) while retention times for geologic formations can be indefinitely. "Subsurface injection of CO_2 into depleted oil reservoirs is a carbon sequestration strategy that might prove to be both cost effective and environmentally safe (Krumhans et al 2002)."

Sequestration of carbon dioxide does have its potential risk. The carbon dioxide when sequestered is preferred to be at the conditions of supercritical state which means that the carbon dioxide will behave as a liquid. CO_2 in the supercritical state is more mobile than petroleum and therefore requires more accurate petrophysical and structural characterization of the rock formations. In order to retain the CO_2 in supercritical state the injection site must be greater than approximately 800m beneath the earth's surface (Basbug et al., 2005). The proposed Wellington Field injection site would be approximately 1500m below the earth's surface towards the bottom of the Arbuckle formation.

Figure 6 shows several different ways of storing CO_2 within a sedimentary medium (Bachu 2003). The most economical option for sequestration of CO_2 would be to directly inject it into hydrocarbon reservoirs as an enhanced oil recovery strategy. Other permanent storage options include: depleted oil and gas reservoirs, deep brine-saturated formations, and deep unmineable coal-beds to remove methane and permanently store the CO_2 (Gunter et al. 2004). Another option would be to store the CO_2 in salt caverns which are currently used to store natural gas.

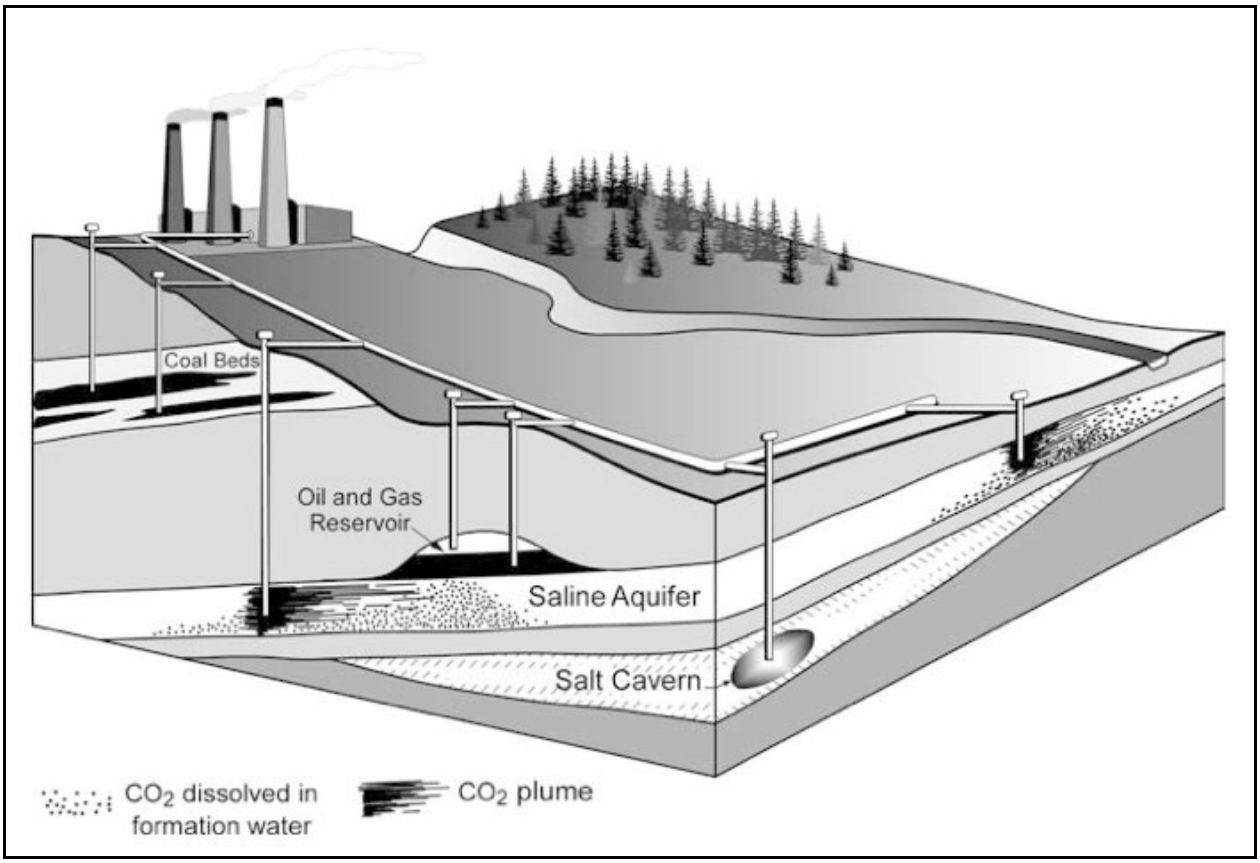

Figure 6 Cartoon showing multiple ways of storing carbon dioxide in geologic formations (Bachu 2003).

Chapter 2 - Geologic Setting and Stratigraphy

Structure

The study area is located in south central Kansas within the Sedgwick Basin. "The Sedgwick Basin, a broad south-plunging shallow embayment of the Anadarko Basin covers an area of about 8,500 square miles in south-central Kansas encompassing 9 counties (Prensky 1997)." The Sedgwick Basin is bound on all sides by other geologic features as seen in Figure 7. To the north it is bound by a small anticline that divides it from the Salina Basin. To the east it is bound by the Nemaha Uplift which separates it from the Cherokee Basin. To the west it is bound by the Central Kansas Uplift which is also an oil producing geologic feature in Kansas. To the south it is bound by the Anadarko Basin.

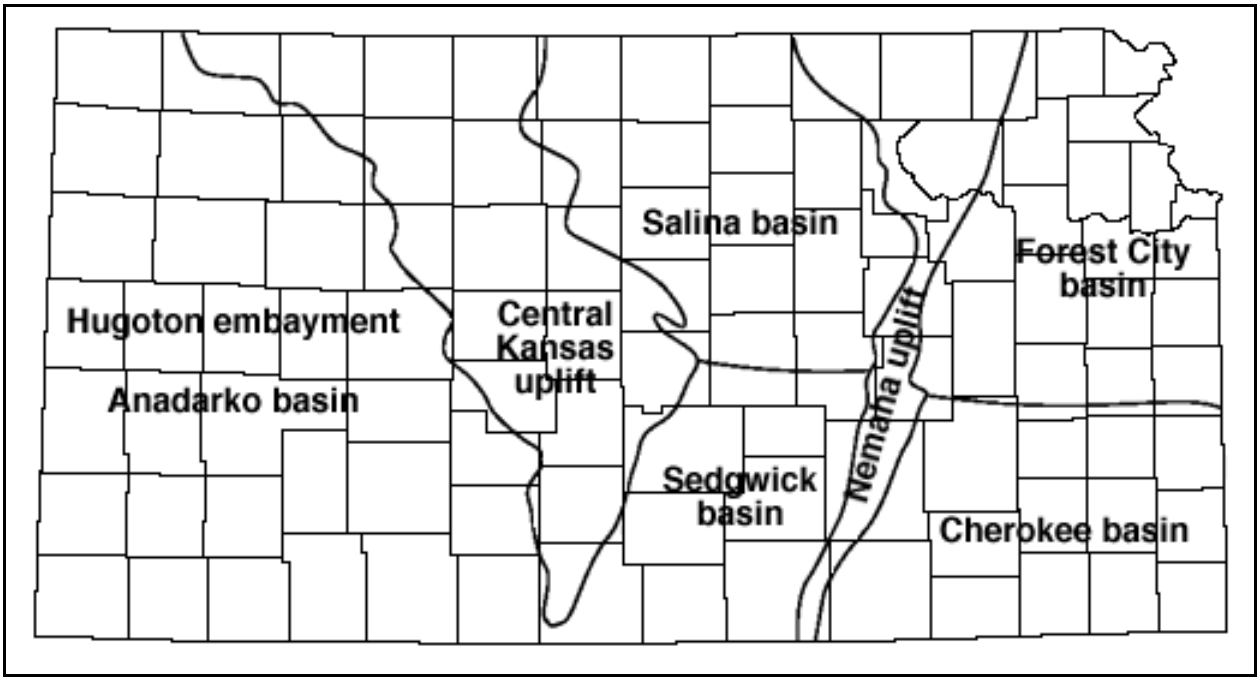

Figure 7 Map of Kansas showing major structural features.

(Figure from http://www.kgs.ku.edu/Publications/Oil/primer09.html)

"Several minor structures, approximately parallel with the Nemaha Anticline, have been recognized in the Sedgwick Basin. These include the Bluff City Anticline, Conway Syncline, Elbing Anticline, Halstead-Graber Anticline, and the southern end of the Voshell Anticline (Merriam 1998)." Precambrian structures throughout Kansas play an important role in the accumulation of hydrocarbons and could also potentially influence the transport of carbon dioxide. Precambrian basement structures are responsible for the formation of structural highs (uplifts) and structural lows (basins) within the state. These inferred structures are visible in Figure 8, as you can see the structures affected by the Precambrian basement are inferred within the study area. Effects from the Precambrian basement structures are seen within the results from this study.

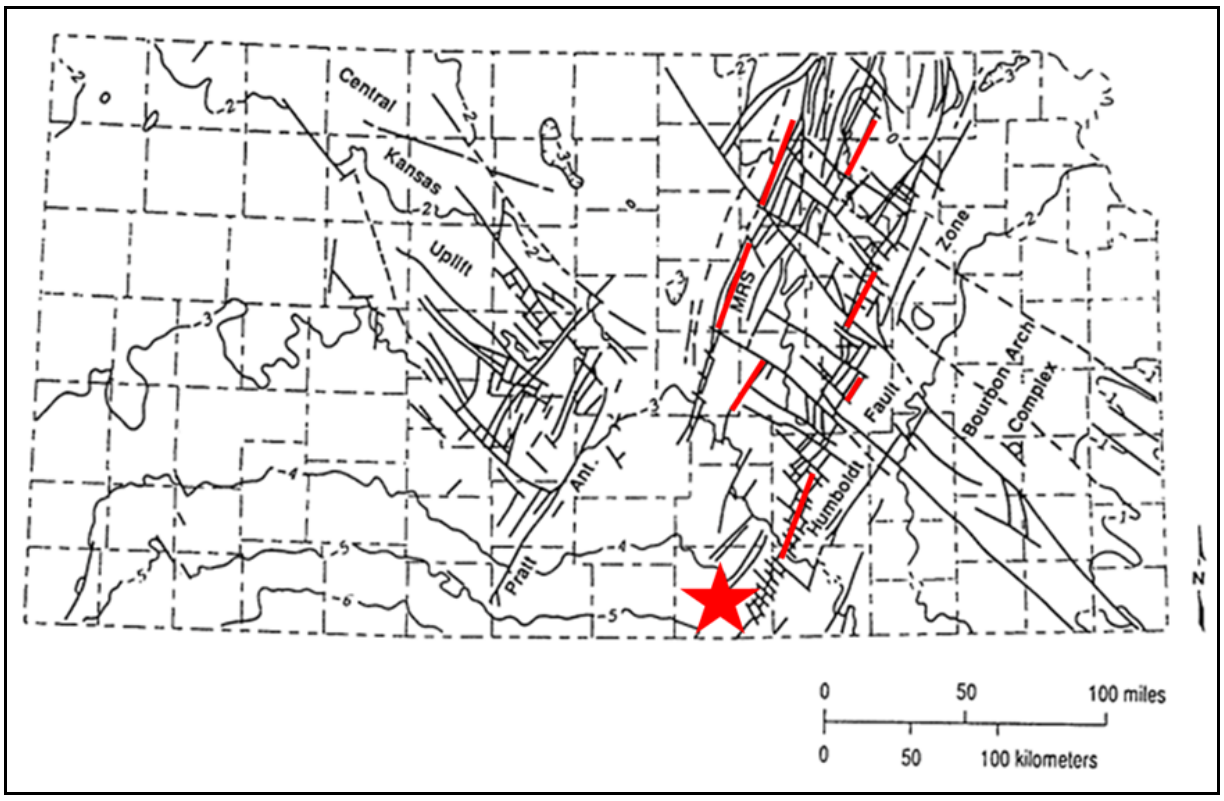

Figure 8 Shows inferred Precambrian basement structures throughout Kansas. The red star is the location of the study area while the red lines are faults associated with the Nemaha uplift. **(http://www.kgs.ku.edu/Publications/Bulletins/233/Baars/)**

The Nemaha uplift may play an important role in the migration of the carbon dioxide plume once sequestered. The Nemaha uplift has been identified as a Precambrian structure by Jorgensen (1989). Faults associated with the Nemaha uplift have a north-east south-west orientation and are known throughout eastern Kansas, as seen in Figure 8. By looking at Figure 8, we can see at least four major faults entering the northern half of Sumner County and predict that any faults or fractures within the study area should be orientated in a similar fashion.

Stratigraphy

Stratigraphy is, defined by the Schlumberger oilfield glossary, the study of the history, composition, relative ages and distribution of strata, and the interpretation of strata to elucidate Earth's history.

The stratigraphy within the Sedgwick Basin was heavily influenced by the surrounding structures. Since the area was part of a south plunging shelf environment leading into the Anadarko Basin, there were frequent sea level changes. With erratic changes in sea level, several different types of sedimentary rocks were deposited. Shales, carbonates, and even chert were able to be deposited in their respective environments. Within the study area, Precambrian basement rock is the only non-sedimentary formation.

This study is focused on characterizing two key formations for potential carbon dioxide sequestration. The Mississippian formation is the primary focus, which is associated with the depleted oil reservoir. While the Arbuckle formation, in this study, is a secondary formation and is associated with the saline aquifer system. The Mississippian formation within the study area is being considered for a pilot carbon dioxide flood to enhance oil recovery. On the other hand the Arbuckle formation is being considered for deep saline aquifer sequestration.

The Mississippian age group, as seen in Figure 9, consists of four separate units: Kinderhookian, Osagean, Meramecian, and Chesterian. This study is concerned with the hydrocarbon producing dolomite lithology that is present in the upper Meramecian and lower Chesterian units. The Mississippian group was deposited as hard parts of calcium carbonate that were produced by marine organisms. These marine organisms lived in a very large epicontinental sea which accounts for the wide spread deposition of Mississippian age rocks (Merriam 1963).

The Arbuckle group is late Cambrian early Ordovician in age, as seen in Figure 9. The study area during this time was part of an epicontinental sea with a warm and humid climate. The dominate sediment deposited was calcareous mud, which later lithified into limestone and was further altered into dolomite (Jorgensen 1989). "The Arbuckle consists mainly of white, buff, light-gray, cream, and brown crystalline dolomite (Zeller 1968)." Chert is possible in the upper portion of the Arbuckle group. The average thickness of the Arbuckle group exceeds 1,000 feet (Zeller 1968). Jorgensen (1989) states that calcareous muds that were deposited in the seas were lithified to limestone, especially during periods of sea recession, and dolomitization then occurred. Dolomitization in this area is assumed to be the result of fresh waters rich in magnesium and calcium mixing with the local marine waters (Jorgensen 1989). The top of the Arbuckle group in this area is at approximately 1200 meters in depth, which is well below the 800 plus meter window for keeping CO_2 in the supercritical state (Friedmann, 2007).

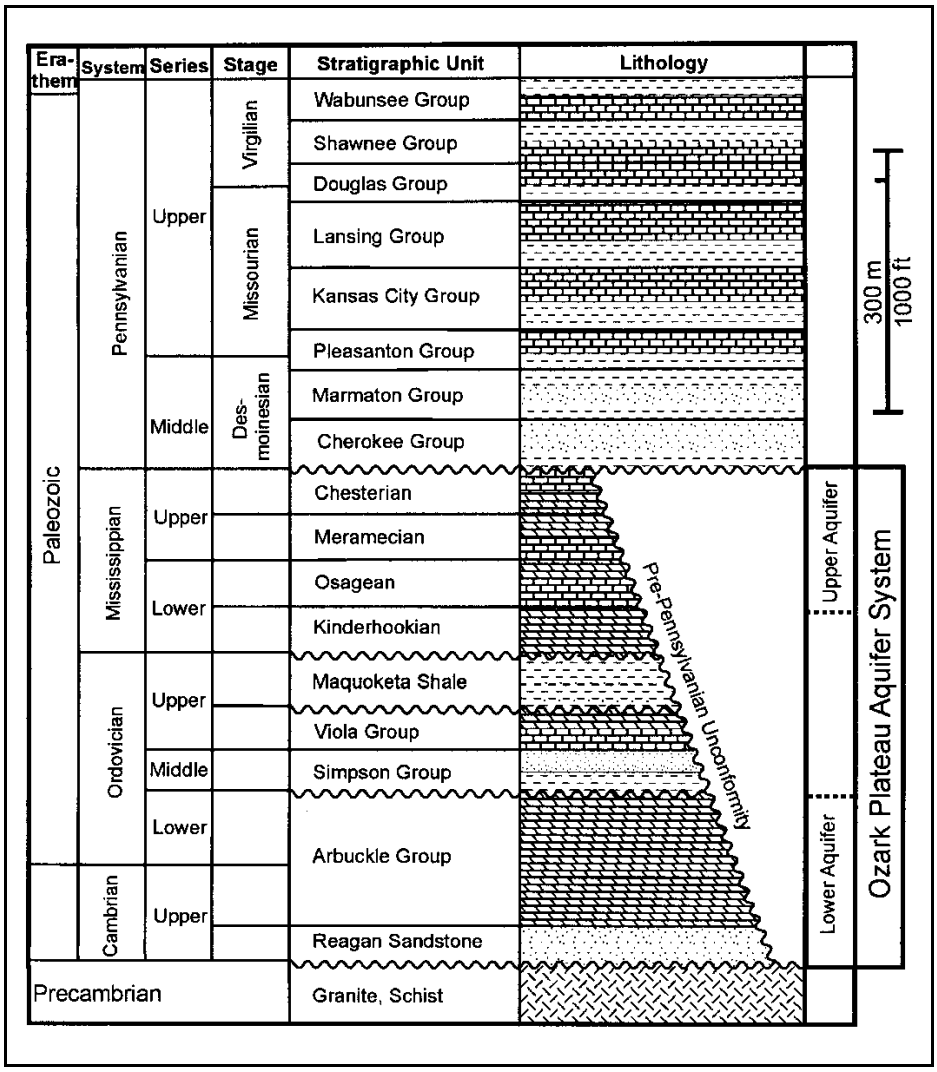

Figure 9 General stratigraphic column of the state of Kansas showing the main formations of study highlighted in yellow (Carr et al 2005).

Sealing formations are vital to the successful application of the carbon dioxide sequestration process. If there is no sealing formation above the injection site, the buoyant carbon dioxide would gradually make its way back to the surface. The major sealing formations in the study area are the Cherokee Shale Member and the Simpson Shale Member, which can be seen in Figures 10 and 11. This study is not focused on the seal formation integrity; this topic would be excellent for future research to compliment this study.

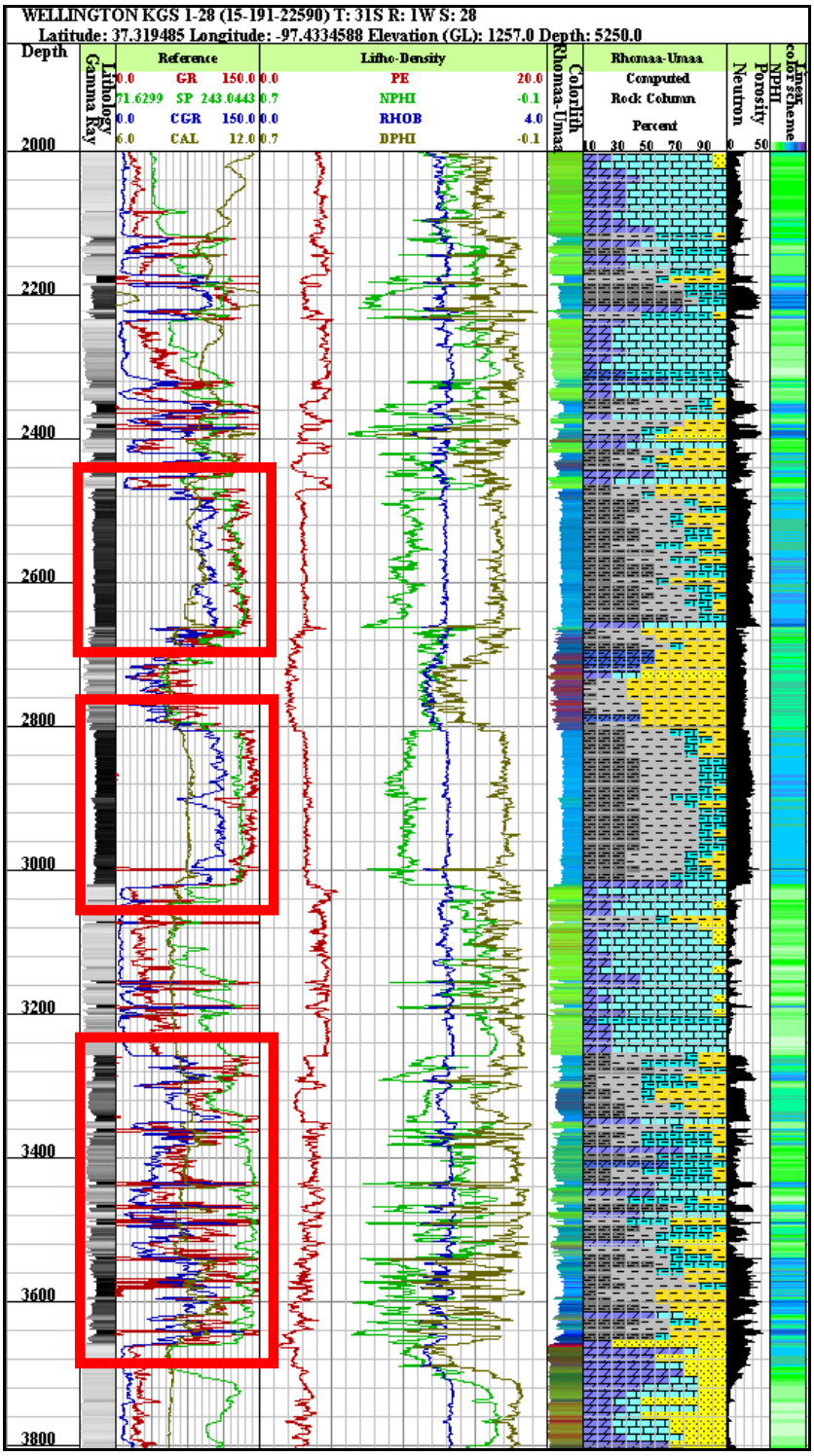

Figure 10 Geophysical well logs (GR-gamma ray, SP-spontaneous potential, CAL-Caliper, PE-photoelectric, NPHI- neutron porosity, RHOB-density, DPHI-density porosity) showing multiple sealing formations above the Mississippian formation. Red boxes show shale members that are potential sealing formations.

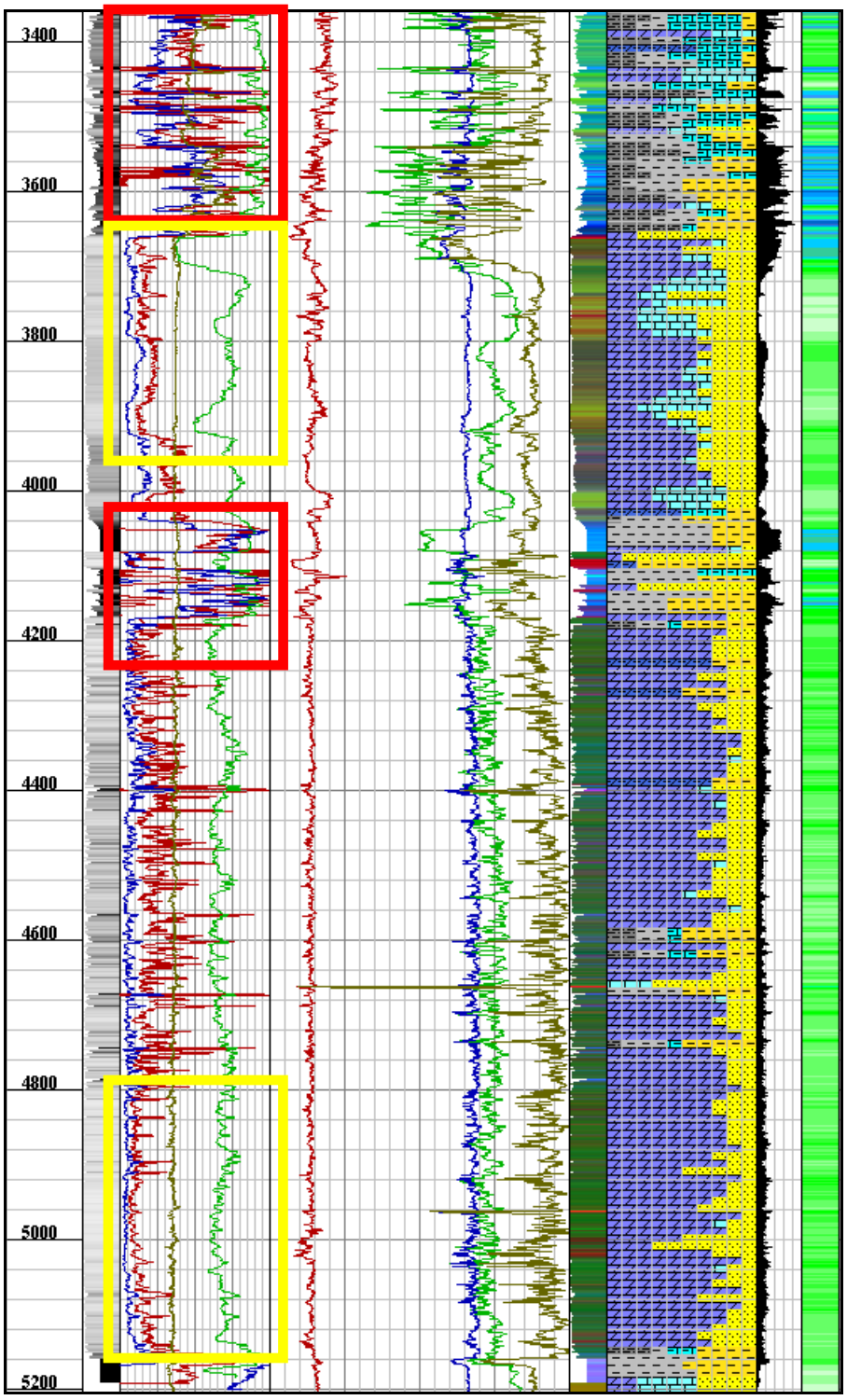

Figure 11 Geophysical well logs (same logs as in Figure 10) showing multiple sealing formations present. Red boxes show shale members that are potential sealing formations. Yellow boxes show formations being considered for geologic sequestration of carbon dioxide.

To fully understand the stratigraphy of the study area, it is important to look at a cross-section view. Figure 12, shows a west to east cross-section of southern Kansas showing the major stratigraphic units and their behavior through the entire southern portion of the state (Merriam 1963). As you can see, the general trend is that the stratigraphic units thicken as you go from east to west. This is expected, as the sediments are being deposited in the Hugoton embayment in western Kansas. Another feature to point out, and may become very important as the DOE project moves along, is the general trend of the formations in Sumner County (Figure 12). The rock formations have a west to east upward trend as they approach the Nemaha uplift. This minor tilt in the rock formations could be very serious if not accounted for, due to the buoyancy of supercritical carbon dioxide.

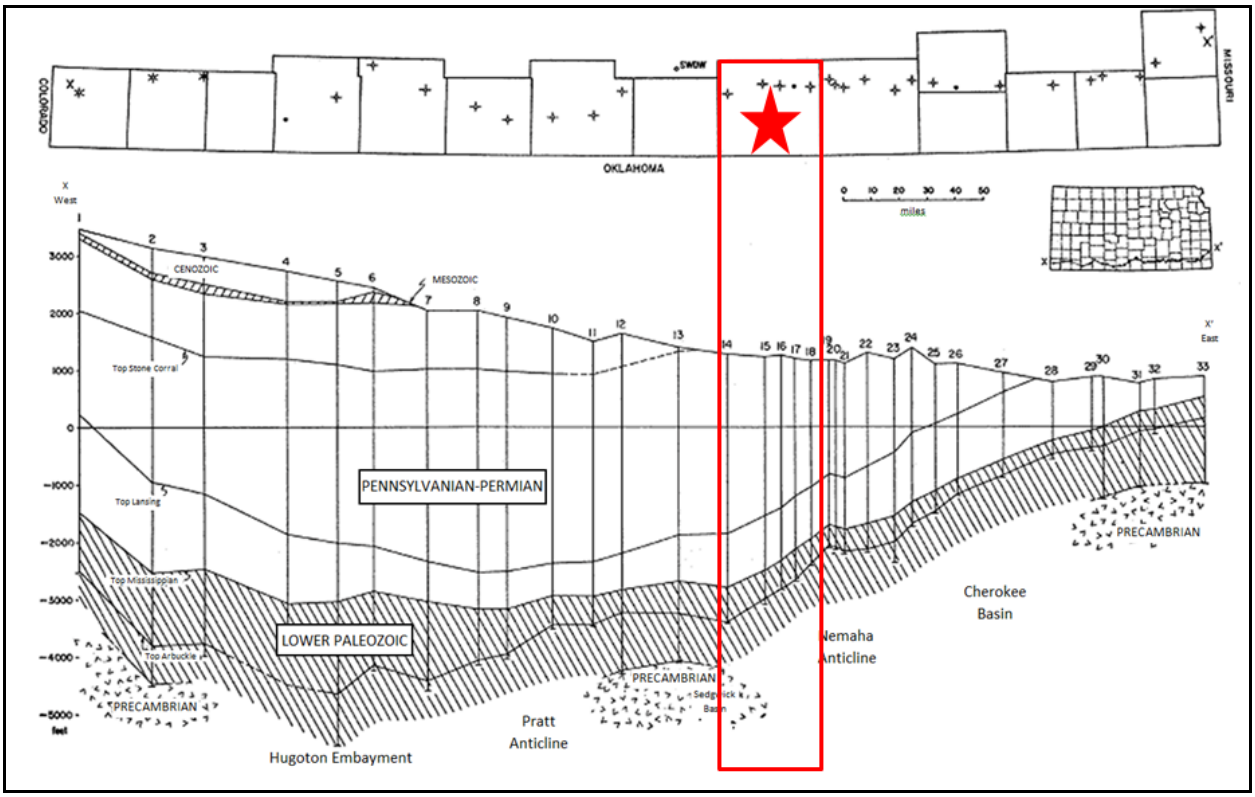

Figure 12 West to east cross-section of southern Kansas showing major stratigraphic units and their general behavior as you move from the Hugoton Embayment in western Kansas to the Cherokee basin in southeastern Kansas. Red box and red star signify the location of the study area. **(http://www.kgs.ku.edu/Publications/Bulletins/162/03_strat.html#Fig5)**

Chapter 3 - Data Acquisition and Methods

Parts of this chapter have been submitted to the Journal of Applied Geophysics (Ohl and Raef, 2012. under review).

3D Data Acquisition

The 3D reflection seismic data was specifically acquired for this carbon dioxide sequestration project by the Department of Energy to help better characterize the subsurface formations. The acquisition of the Wellington Field 3D seismic took place in March/April of 2010. The acquisition was executed by Paragon Geophysical Services out of Wichita, Kansas. Some of the specs used during the acquisition are as follows: ION Scorpion recording system (Figure 13), single three component (3C) Digital geophone (Figure 14), source and receiver interval was 165 feet, receiver line interval was 495 feet, source line interval was 660 feet, two 62,000 pound vibrators were used as the seismic source (Figure 15), the sweep parameters were four sweeps at twelve seconds with a recording length of five seconds. The vibroseis sweep included energy in the range of 16 to 130 Hz. Figure 16 outlines the area of the survey in green. The blue outline in Figure 16 is the Anson-Bates 3D seismic data that was purchased from Nobel Energy and then merged with the Wellington field 3D data.

Figure 13 Shows the Paragon Geophysical Services recording station. Figure 14 Shows the single 3C Digital geophone planted in the ground ready for listening.

Some other survey parameters were; 288 in-lines and 178 cross-lines. The sampling rate for the survey was two milliseconds, while the recording length was five seconds. Echo Geophysical Corporation and Fairfield Nodal where responsible for processing the raw seismic data. The processed data files reached Kansas State University in the summer of 2010 and where loaded into an interpretation project in Kingdom Suite software (licensed by Seismic Micro-Technology, Inc.) in August of that year. Fifty five wells and their respected logs were also imported into Kingdom Suite project for assistance in the seismic analysis and reservoir characterization process.

Figure 15 Shows the two vibroseis sources used to acquire the seismic data.

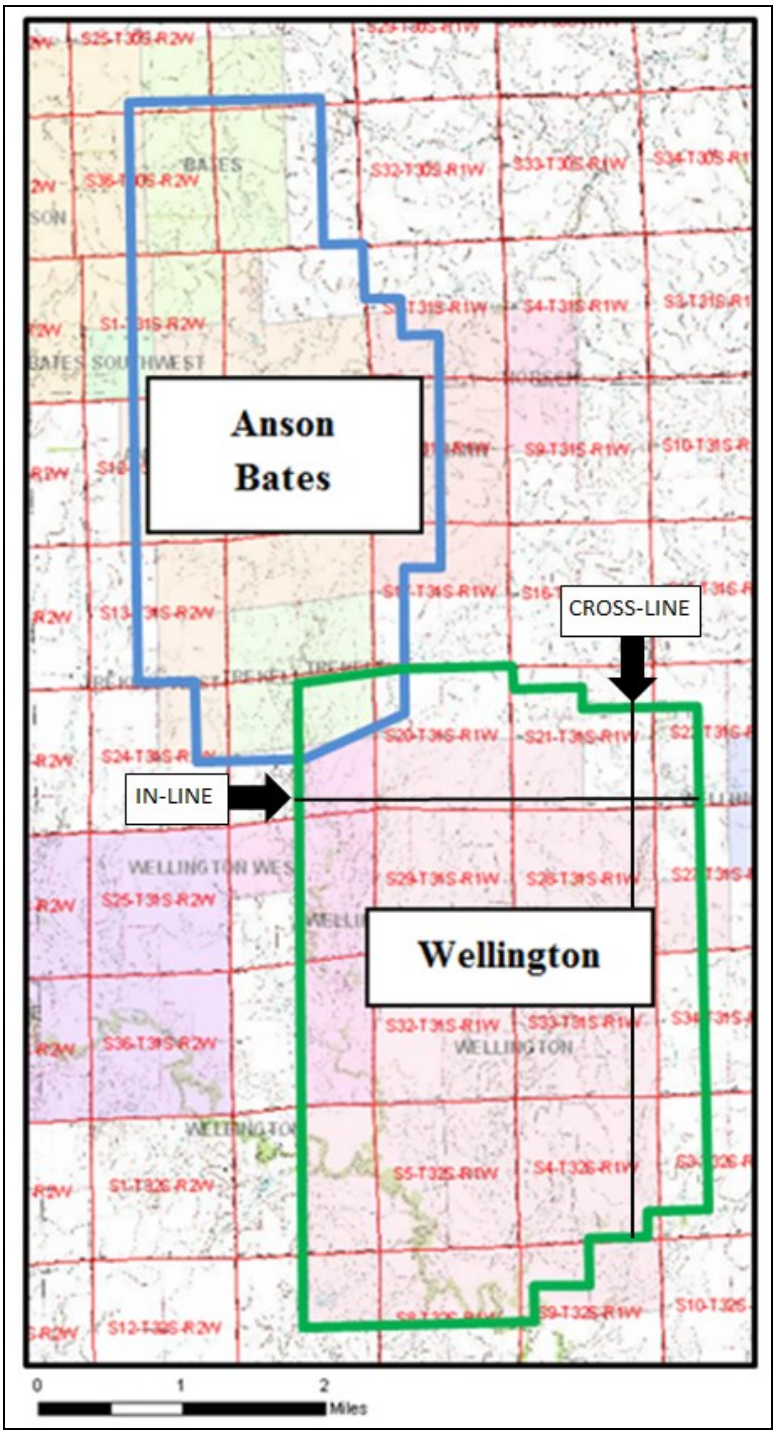

Figure 16 Showing the outlines of the two 3D seismic surveys. Green is the outline of the Wellington 3D and the blue outline is for the Anson-Bates 3D survey. (Picture modified from the KGS)

Interpretation Methods

Synthetic Seismic Modeling

Quality synthetic seismograms are vital to accurately interpret seismic data. Synthetic seismograms allow the interpreter to correlate geophysical well logs, sampled in feet, with the seismic data, sampled in the time domain. This step in the seismic interpretation process helps to build time-depth tables that help linking-up between the two domains and allows the interpreter to cross-plot well logs and seismic data attributes. More importantly, upon completion of a good synthetic-to-seismic tie the interpreter would be able to match seismic events to the corresponding stratigraphic tops.

Synthetic seismograms are generated using sonic and density logs to calculate the reflection coefficient which can be seen in Equation 1. Once the reflection coefficient for the sonic and density logs is calculated then a seismic wavelet, which is extracted from the seismic data around the wells borehole, is convolved by the calculated reflection coefficient in order to yield a synthetic seismogram (Equation 2). Convolution is the process of joining together two functions to produce a third function. In the case of a synthetic seismogram, the seismic wavelet that is extracted from the seismic data is convolved with the reflection coefficient to produce the synthetic seismogram.

$$e(t) = \frac{V_2\rho_2 - V_1\rho_1}{V_2\rho_2 + V_1\rho_1}$$

Equation 1 Where V is velocity and ρ is density. The change in velocity and density between two mediums gives the reflection coefficient. V_1 is velocity in medium one while V_2 is the velocity for medium two. ρ_1 is the density for medium one while ρ_2 is the density for medium two.

$$x(t) = w(t) * e(t)$$

Equation 2 Where w(t) is the seismic wavelet which is multiplied by the reflection coefficient e(t) to produce a synthetic seismogram x(t). (t) signifies time. The $*$, signifies the convolution process.

Figure 17, shows a raw synthetic seismogram before any editing has been done. It is important to note that the synthetic seismogram (in the third column from the right) has a very low correlation factor (r circled in red) which means that the correlation between the synthetic seismogram and the seismic trace extracted from around the borehole is low. Editing the synthetic seismogram by correlating reflectors with one another will yield a higher correlation factor and more accurate tie between the seismic data and the well log data (Figure 18). This tie between the seismic data and well logs allows the interpreter to associate seismic peaks or troughs with certain geologic formation tops.

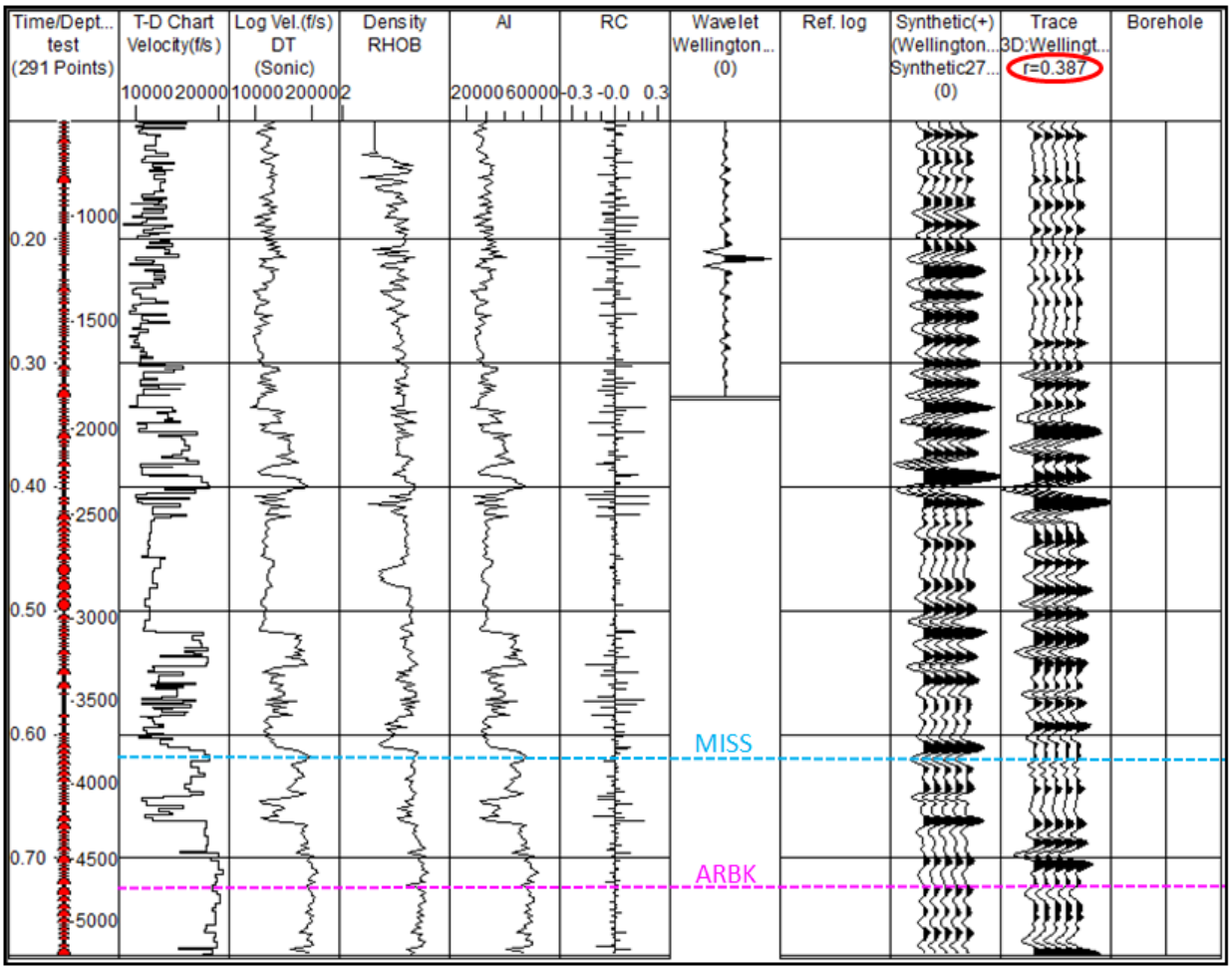

Figure 17 Raw synthetic seismogram for the Wellington KGS 1-28 well.

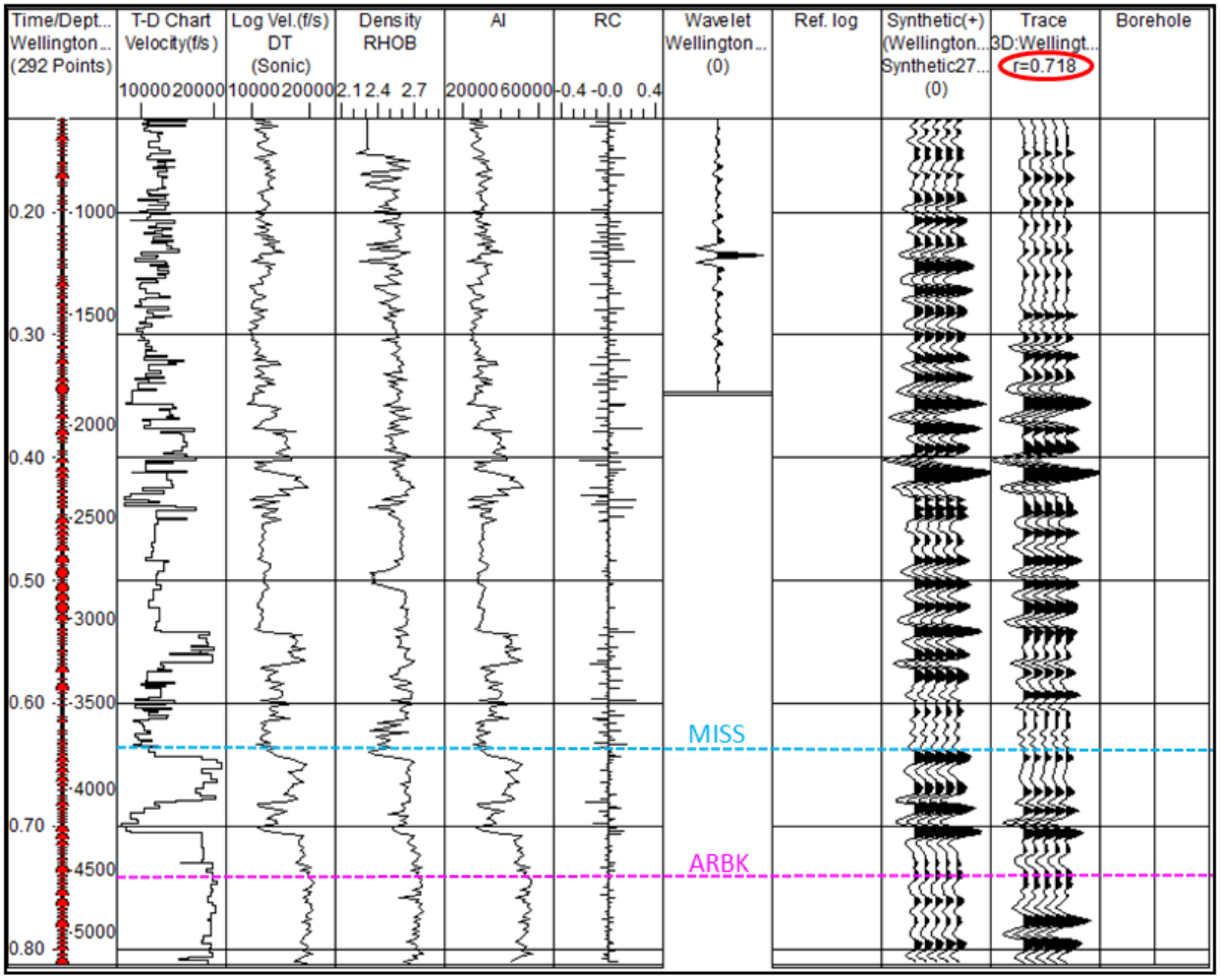

Figure 18 Edited synthetic seismogram for the Wellington KGS 1-28 well.

In the synthetic seismic modeling of this study a replacement velocity of 10,000 ft/sec was used for the difference between the seismic datum (1300 ft.) and the start depth of each sonic well log for six wells within the study area. Special attention has been paid to matching based on seismic wavelet character and avoiding any excessive use of "stretch-and-squeeze". Average cross correlation coefficient between real seismic data around wells and synthetics is 0.7. Most of the miss-tie (about 30 % on average) is attributable to a phase mismatch of the real seismic-data wavelet, which is of mixed phase (Ziolkowski et al., 1998) and the zero-

phase/constant phase wavelet used in the convolution with the reflectivity function, which was calculated from well logs, e.g. (Henry 2000).

The added advantage from a direct correlation with borehole logs is that there is an actual measurement of depth against which the seismic section can be constrained (Reynolds 1997). Stratigraphic tops, established from geologic drilling reports, of the Mississippian and Arbuckle groups were used in identifying events to be tracked as time horizons after achieving good quality synthetics-to-seismic tie at six wells.

Horizon Tracking

Horizon tracking was done using a combination of synthetic seismograms as well as individual well data. Horizon tracking is the process of using synthetic seismograms to map rock formation tops in order to see subsurface stratigraphy throughout the seismic data. Formation top data for each well was input into Kingdom Suite Software. This formation top data correlated with the synthetics helped determine the placement of the horizons as seen in Figure 19. If the formation top (after generation of the synthetics) was associated with a synthetic peak or trough than the corresponding horizon was tracked along that same peak or trough. The horizons were picked manually to insure the best possible formation top. Auto picking horizons has the capability of skewing the horizon because it picks within a window restriction and does not always continue picking the correct reflector. This is most prevalent when the amplitude of the reflector varies throughout the survey. It is because of these issues that auto tracking of the horizons was not used in this study. Having these key formation tops picked allows us not only to create maps along that surface, but allows us to see subsurface stratigraphy within the seismic data. This is important because 3D seismic data is in time not depth.

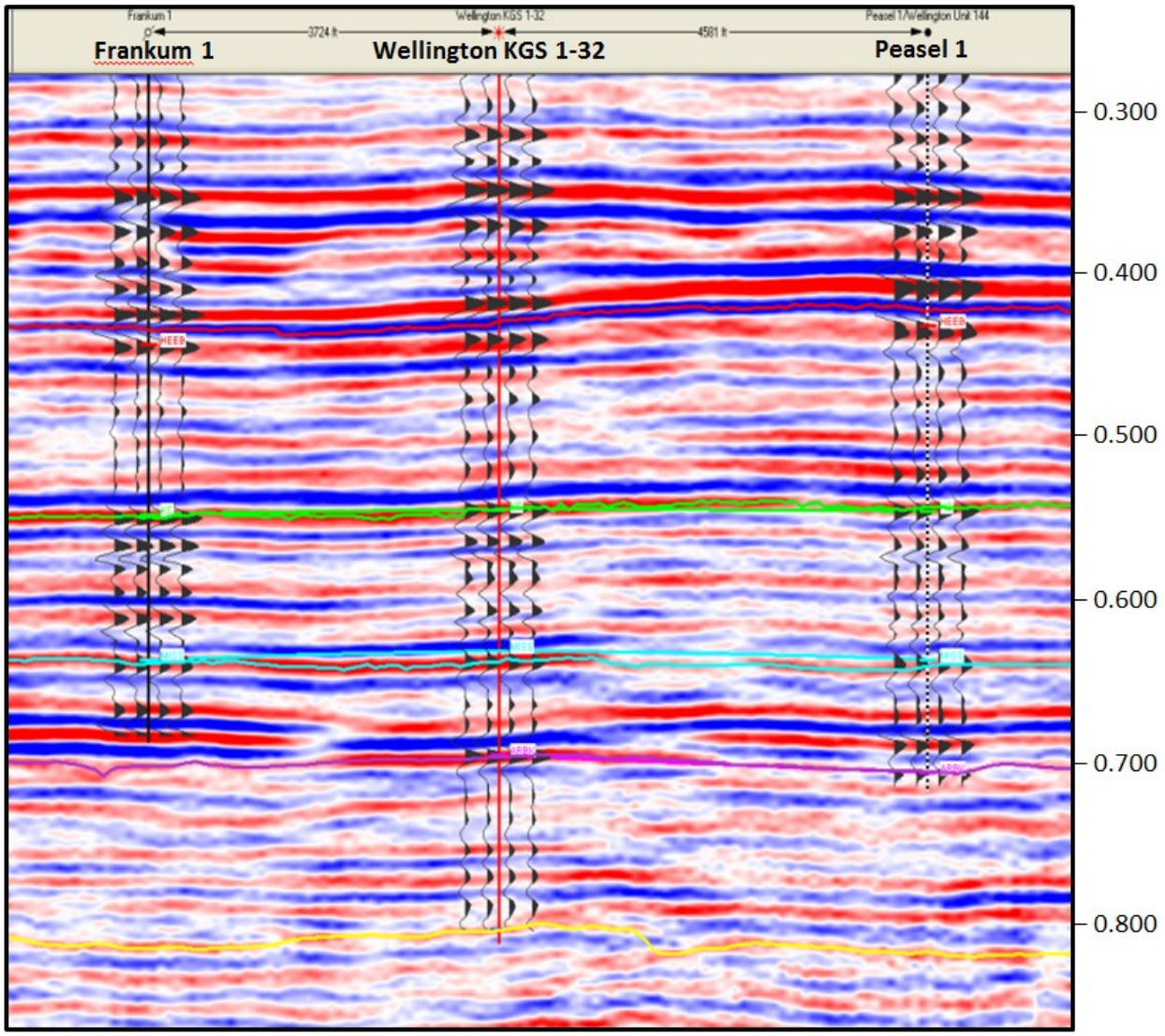

Figure 19 Seismic amplitude section with tracked time horizons (depicted by the red (Heebner), green (Kansas City), blue (Mississippian), purple (Arbuckle), and yellow (Basement) lines) corresponding to those formation tops. (Ohl and Raef, 2012. Journal of Applied Geophysics, under review)

Seismic Attributes

Seismic attributes have been helping geophysicists predict lithological and petrophysical properties of oil and gas reservoirs since the early 1970's (Chopra and Marfurt 2008). Seismic attributes have also been used effectively in many reservoir characterization, CO_2-EOR and/or carbon sequestration monitoring tasks, e.g., Arts et al. (2002); Raef et al. (2005), Raef and Slusarczyk (2001); Chopra and Marfurt (2008); and Lozano and Marfurt (2008). In this study, we use key attributes such as: amplitude, coherency, and curvature. These seismic attributes will then be cross-correlated in order to characterize the Mississippian and Arbuckle formations for carbon dioxide sequestration. During the attribute analysis process, extra attention is given to small details from structure sensitive attributes, namely coherency and curvature, in order to determine the most complete structural model. It is these small scale features that could potentially cause derailment of flow simulation modeling if they are not accounted for.

Seismic interpreters may have a difficult time distinguishing shale filled channels vs. sand filled channels without attribute-assisted interpretation (Suarez et al., 2008). It is also difficult to distinguish small-scale, below seismic resolution, channels and faults, especially when both would be evident in the form of amplitude dimming. These challenges are the reason why, in this study, multiple seismic attributes are being interpreted together in order to yield the "most" accurate interpretation of the subsurface within the study area.

Amplitude

Fred J. Hilterman (2001), states that seismic amplitude is now one of the major criteria for recognizing potential hydrocarbon reserves. Seismic amplitude depends on reflection coefficient or reflectivity, which in turn depend on impedance contrast as shown by Equation 1. Bright spots within seismic data are characteristic of hydrocarbon producing zones, but dimming

of seismic data has also been associated with some hydrocarbon zones in the industry. Seismic amplitude can also detect and show the oil-water contact or gas-liquid contact within a structurally trapped hydrocarbon reservoir (Hilterman 2001). When planning to drill a well, knowing where the oil-water contact is would allow for proper drilling and completion techniques in order to produce the most hydrocarbons possible before taking on water. Post-stack seismic amplitude anomalies have also been used successfully in mapping channel sands, e.g. Harilal and Biswal (2010).

Variation in seismic amplitude can be caused by several factors such as lithology, change in porosity, pore fluid composition, and thickness of rock formations. High saturations of oil and/or gas within the reservoir rock can have both positive and negative effects on seismic amplitude. Positive effects on seismic amplitude, due to hydrocarbons, are known as bright spots and can be used as direct hydrocarbon indicators. On the other hand, hydrocarbons can have a negative effect on seismic amplitude. These negative effects are known as dim spots or seismic dimming. Seismic dimming, only when the cap rock has lower impedance than the reservoir rock, can also be used as direct hydrocarbon indicators (Bacon et al., 2003).

In addition to the previous factors, scattering and interference due to morphology of the geo-bodies could cause a change in amplitude. Lens shaped channel sands or irregularities of reflectors due to small throw faults or carbonate buildups can also cause amplitude anomalies. Absorption of seismic amplitude, which would be displayed as seismic dimming, also occurs when the seismic energy passes through a salt body. It is these types of changes within seismic amplitude that makes amplitude, by its self, a difficult attribute to use in the seismic interpretation process. The interpreter must use other seismic attributes in order to fully understand why the seismic amplitude is a bright spot or an area of dimming.

"In many cases, lateral amplitude changes are related to changes in porosity rather than fluid fill. This is particularly true for well-consolidated sands and carbonates (Bacon et al., 2003)." This section of Bacon et al. gives insight into certain amplitude anomalies seen within the study area. These amplitude anomalies will be discussed further in the results and discussion section which will follow this chapter.

Coherency

The coherency attribute was introduced by Bahorich and Farmer (1995) as a usable interpretation seismic attribute that they defined as a quantitative measure of the similarity or dissimilarity of nearby seismic traces (Equation 3). Comparison of the seismic coherency attribute with conventional horizon based structural attributes, namely time dip, azimuth, and dip azimuth, has concluded that one of the significant merits of the seismic coherency attribute is its robust volumetric pattern of calculations that is independent of the interpreter and auto-picking biases. The seismic coherency attribute has been established as a sensitive responder for delineating geologic faults as well as considerably more subtle stratigraphic features such as: channels, canyons, and slumps (Marfurt et al., 1998).

$$\Phi(t,d) = \frac{\sum_{k=t-N/2}^{k=t+N/2} G_k H_{k+d}}{\sqrt{\sum_{k=t-N/2}^{k=t+N/2} G_k^2 \sum_{k=t-N/2}^{k=t+N/2} H_{k+d}^2}}$$

Equation 3 Where Φ is the correlation coefficient at time (t) (milliseconds) for a specific geologic dip (d). G and H are the correlated traces and N is the number of samples in the correlation time window.

The seismic coherency algorithm compares waveforms from multiple traces around each individual trace, as seen in Figure 20. Each single trace, the pink trace in Figure 20, is compared to all the surrounding traces (green traces). This method of calculating coherency is the most robust, yielding the highest quality coherency maps. Other, less robust, coherency algorithms only use three seismic traces to compare, instead of using the five traces in the higher quality calculation. Comparing four traces around each single trace assures that the attribute will see more changes in waveform, allowing the interpreter to see more small scale structural features.

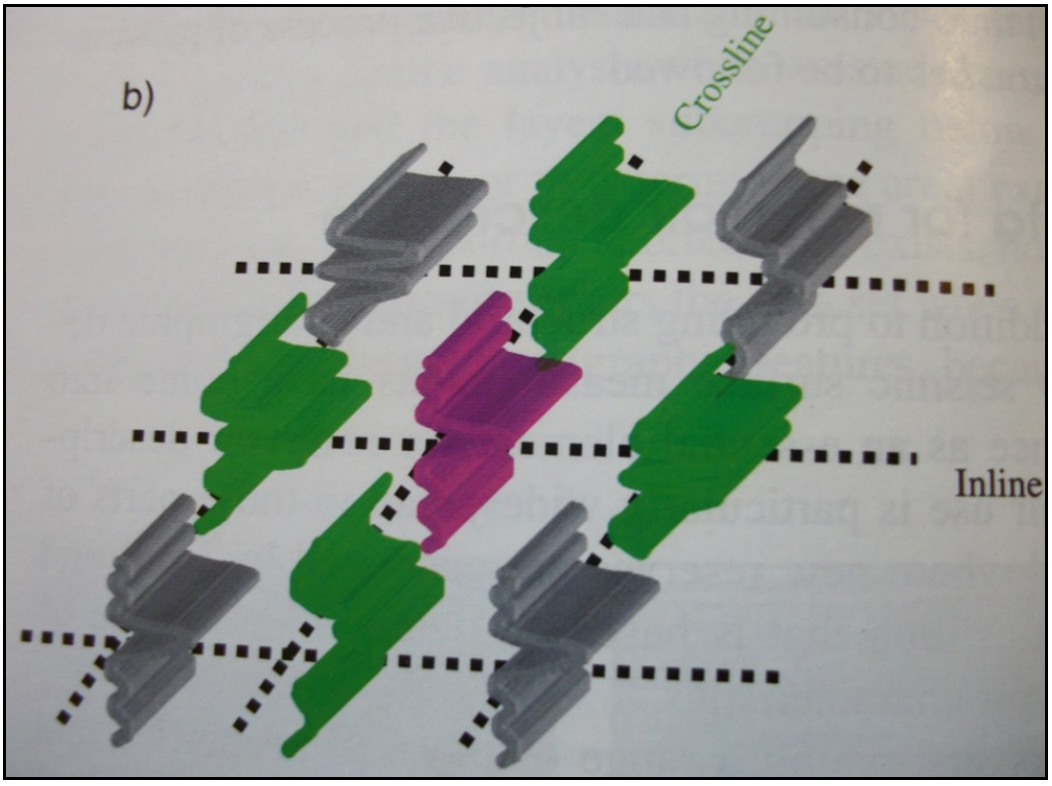

Figure 20 Coherency attribute comparing multiple seismic traces around a single trace. (Chopra and Marfurt, 2007)

Curvature

Curvature was accepted as a means of predicting fractures from surface seismic data following a study by Lisle in 1994, where Lisle correlated curvature values to fractures measured on an outcrop (Chopra and Marfurt 2007). The definition of curvature is the radius of a circle

tangent to a curve. Curvature is used to aid the coherency interpretation looking at structural features such as faults and channels. As you can see from Figure 21, curvature is separated into three types; positive curvature is associated with anticline features, negative curvature is associated with syncline features, and zero curvature is associated with linear features. Curvature is a seismic attribute that is sensitive to faults and fractures within rock formations. Curvature utilizes dip and azimuth calculations from the seismic data which are very sensitive to changes in structural properties within the rock formations. For example, a fault with throw greater than the seismic resolution will have a greater curvature signature than a fault with throw less than the seismic resolution.

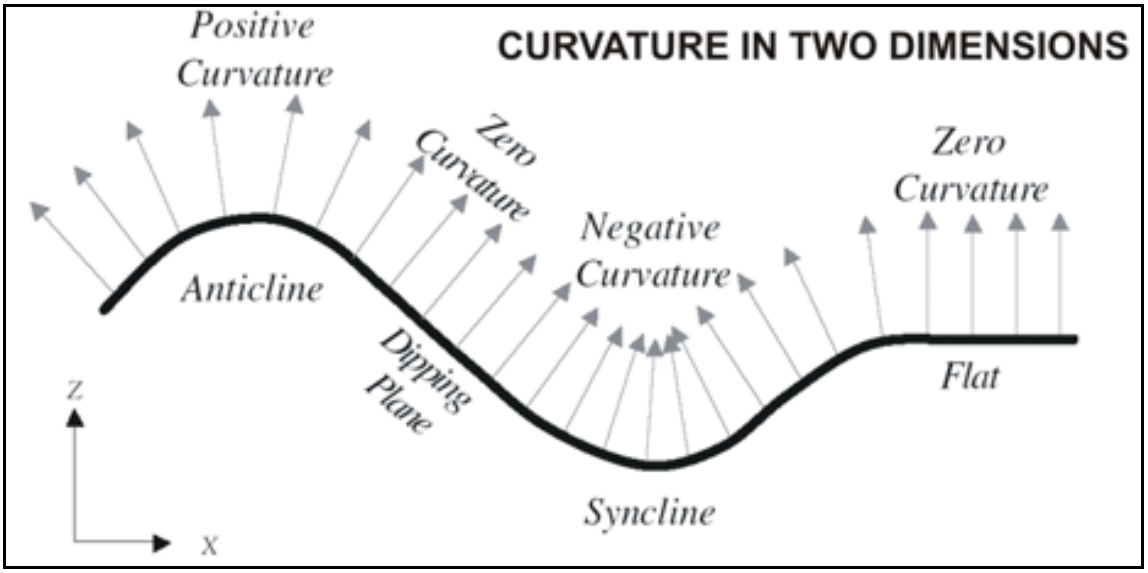

Figure 21 Diagram showing 2D curvature along a reflector; positive curvature is associated with anticline features, negative curvature is associated with a flat surface or dipping plane, and zero curvature is associated with syncline features (modified from Roberts 2001).

In this study most negative curvature attributes were calculated for the entire 3D seismic volume allowing no bias from using a certain window. By calculating maximum positive or maximum negative curvature the maximum positive and/or negative bending of the subsurface at

a given point is determined (Chopra and Marfurt 2007). These two curvature attribute calculations are most useful when looking at structural lineaments. These structural lineaments are often associated with faults, fractures, or channel sands.

Seismic Petrophysical Facies Modeling

Optimized reservoir/aquifer characterization needed for CO_2 based enhanced oil recovery or geological sequestration requires integrating various datasets; time lapse and 3D seismic data, well logs, and core sample measurements and description. Seismic petrophysical facies modeling was incorporated into the study to look at petrophysical facies effects on 3D seismic attributes. Modeling was undertaken to help clarify amplitude and coherency anomalies seen within the study area. With the added information from integrating well log information with seismic attributes, the modeling section of the study was focused on looking into the importance of porosity throughout the entire 3D seismic survey. Since porosity can have a direct effect on amplitude, it was important to try and model changes in porosity throughout the survey with limited porosity data.

Figure 22, is a schematic showing the basics of how neural networks work. Any number of variables can be input into the neural network as input layers. These input layers are then cross-correlated with hidden layers. Hidden layers are layers of data that are used to restrict the correlation between the input layers. After correlation between the two layers has occurred, then an output prediction is made. For this study the input variables are seismic attributes, while the hidden layers are well log porosities. Correlating these two data sets yields a porosity classification map based on seismic waveform attributes and well log porosity.

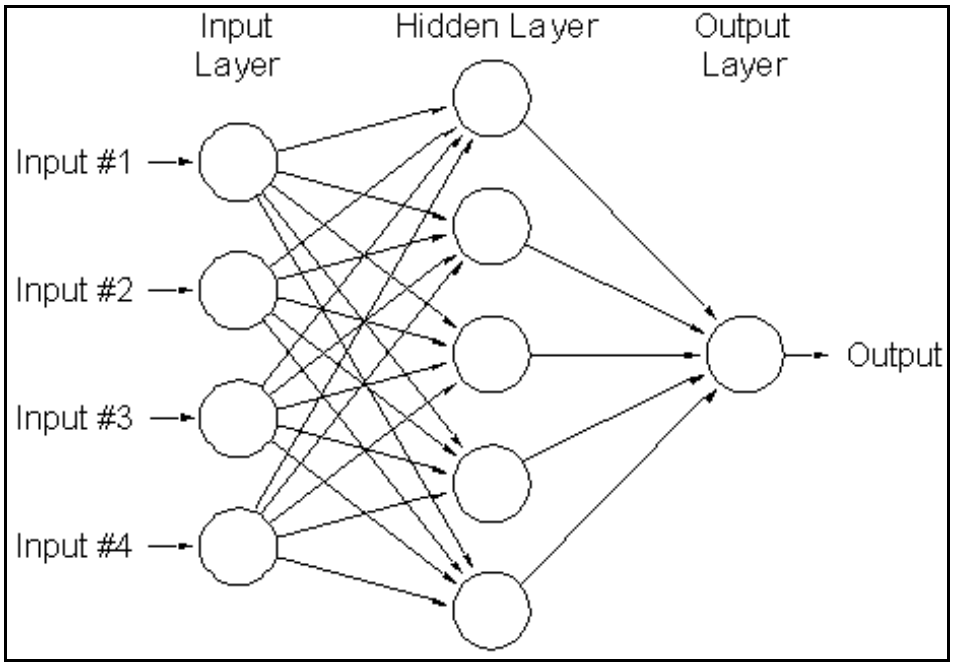

Figure 22 Schematic demonstrating the process of neural network correlation between input layers and hidden layers to produce an output layer. In the case of this study, waveform attributes were the input layer while well log porosity classes were the hidden layer to produce the petrophysical facies map. (psycnet.apa.org)

Artificial neural network classification of 3D seismic waveform, when guided with lithofacies and/or petrophysical properties from core samples and borehole measurements, offers a practical and robust approach of mapping petrophysical facies (Cortis et al., 2008; Russell et al., 2003; Saggaf et al., 2003; West et al., 2002). The artificial neural network used to classify the waveform used the supervised method, which restrains the neural network calculation to the input pick sets. Three wells were used as the pick sets to help supervise the training of the neural network.

The input layer for the artificial neural network is comprised of three seismic attributes: energy, band width, and peakedness of the seismic wavelet of the Mississippian horizon. Energy, band width, and peakedness seismic attributes, were extracted utilizing OpendTect, which is an

open source seismic data analysis software provided by dGB Earth Sciences B.V. Matlab R2008B of MathWorks was utilized in applying the artificial neural network training, validation, and application. Later OpendTect was used for further validation of the neural network process and application to the study areas seismic data. These results will be discussed in the next chapter.

Well log porosities were used to explore petrophysical facies classes within the study area. Well log porosities for most wells having porosity logs in the study area are shown in Figure 23. There seems to be a wide variety of porosities within the study area. Porosities were separated into three different classes; high (12+ percent), intermediate (8-12 percent), and low (below 8 percent) porosities. Indicating petrophysical facies based on the porosity classification was a preparation step in building learning vectors. That was used in a learning vector quantization which is a method for training competitive layers in a supervised manner. Three petrophysical classes/facies were identified based on well log porosities and used as target classes in the training and validation stage of the competitive neural network. Class one petrophysical facies has high porosity, class two petrophysical facies has intermediate porosity, while class three petrophysical facies has low porosity.

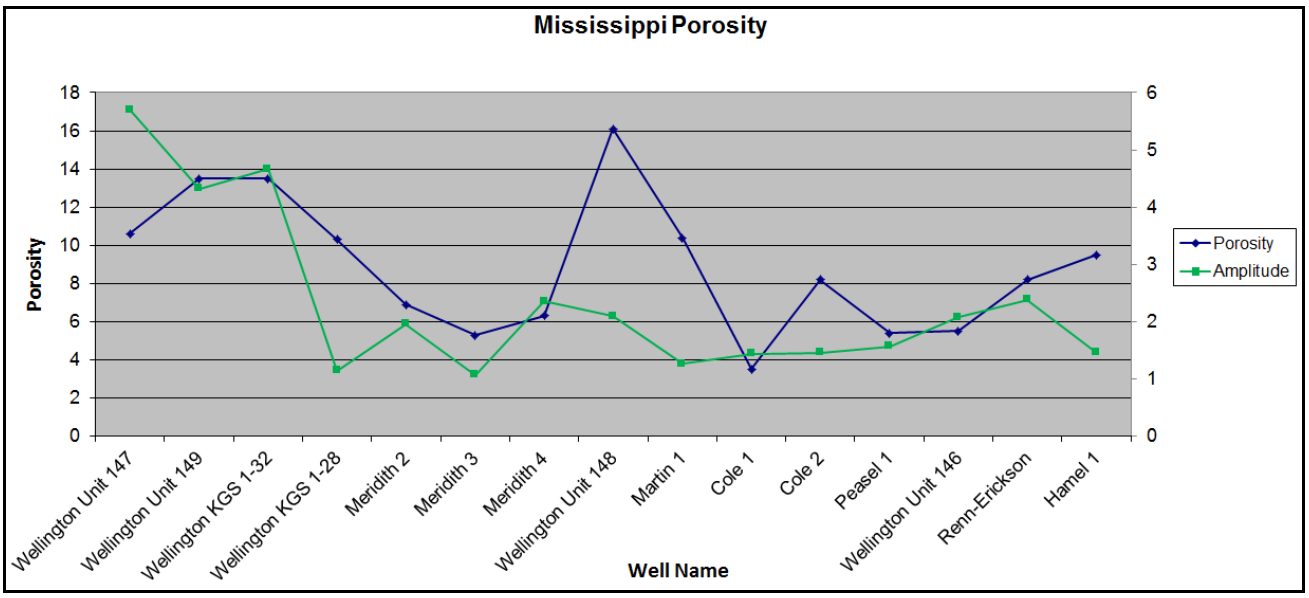

Figure 23 Average Mississippian porosities and seismic horizon amplitude for the Mississippian top. Seismic amplitudes show some correlation with Mississippian porosity.

The concern about using neural networks to aid in the characterization of rock formation properties is summed up in a paper by Kalkomey et al., 1997. In the paper, the authors are concerned how seismic attributes are selected to be used in the neural networks and suggest using as many seismic attributes as possible. If too few seismic attributes are used, then the neural network correlation between the attributes and the well logs could be skewed and possible miss interpretation of the seismic data could occur. The seismic attributes used in the training and application of this study are all waveform based and would most resemble changes in lithology. Further work expanding the neural network would be a great compliment study. Exploring different neural networks based off of different seismic attributes could potentially lead to greater understanding of seismic anomalies seen within the study area.

Chapter 4 - Results and Discussion

Parts of this chapter have been submitted to the
Journal of Applied Geophysics (Ohl and Raef, 2012. under review).

Mississippian Characterization

In this case study of the Wellington and Anson-Bates hydrocarbon field in south central Kansas, dimming amplitude anomalous features (Figure 24) have been interpreted along the upper portion of the Mississippian reflector within the seismic data. These anomalies trend north-northeast-south-southwest (NNW-SSW) which is the same trend of known features associated with the Nemaha Uplift (Figure 8). This resemblance builds the suspicion of these features being associated with the regional effects from the Nemaha Uplift.

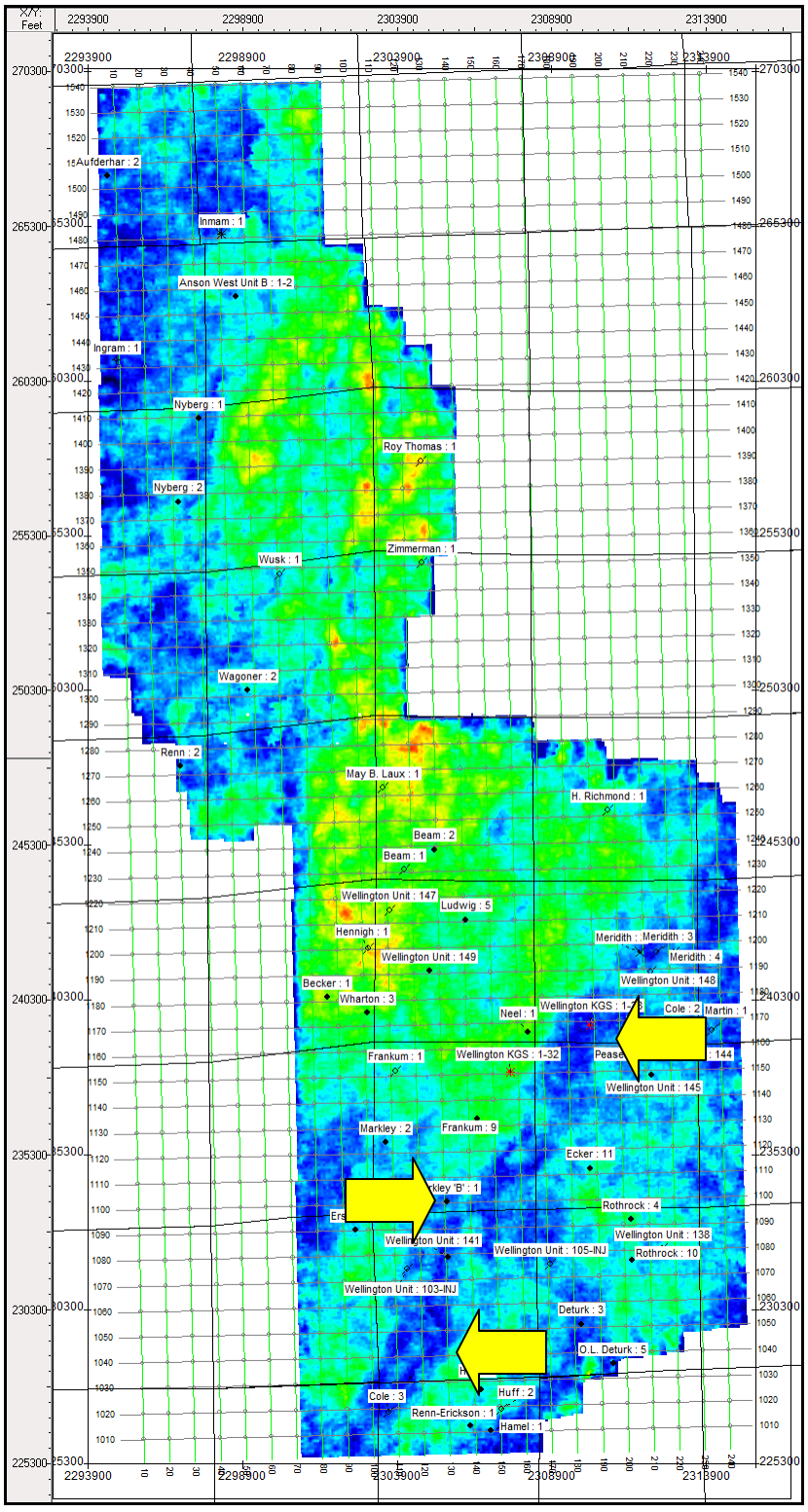

Figure 24 Mississippian horizon showing seismic amplitude variation. A large anomalous feature is seen trending NNW-SSW and is pointed out by arrows.

Since there is an anomalous feature within the seismic data we must determine if the feature is real or some type of artifact associated with the seismic data processing. The first step was to look into the signal to noise ratio of the data within the anomalous feature. Figure 25 shows the signal to noise plot extracted from within the feature. Compared to the entire spectrum taken from the Wellington 3D seismic data set (Figure 26) there is very little change between the two spectrums and therefore the anomalous feature is not an artifact from processing techniques used.

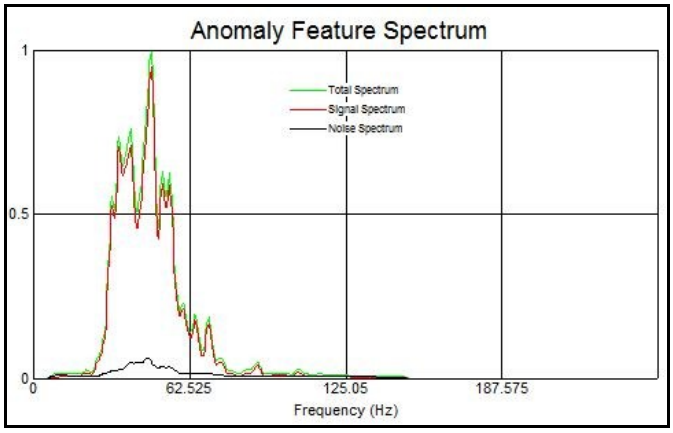

Figure 25 Shows the signal to noise spectrum extracted from the anomalous area.

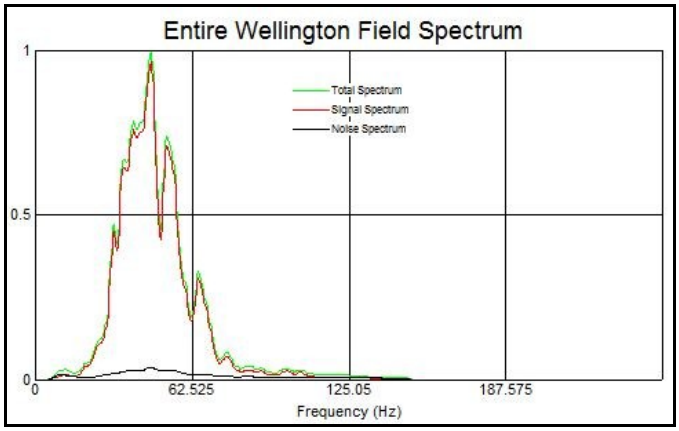

Figure 26 Shows the extracted signal to noise spectrum for the entire survey. It is important to note the similarity between the two spectrums and as a result the anomaly is not an artifact.

The spatial span of the amplitude anomaly and amplitude dimming also points to two equally possible interpretations: first, a lens shaped incised meandering channel sand, while the second interpretation is a small-scale faulting system with resulting changes in porosity. Figure 27a shows Mississippian horizon amplitude map with a linear anomalously low zone trending NNE. The interpretation that upward extensions of rejuvenated basement faulting with little throw and subsequent reworking along fault escarpments is the most likely interpretation, especially in the light of recent drilling of the Wellington KGS 1-28 well. During drilling of the Wellington KGS 1-28, the onsite geologist examined a reworking of the top of the Mississippian formation. This reworking of the Mississippian formation has yielded change in the porosity of the formation and also has increased the amount of chert.

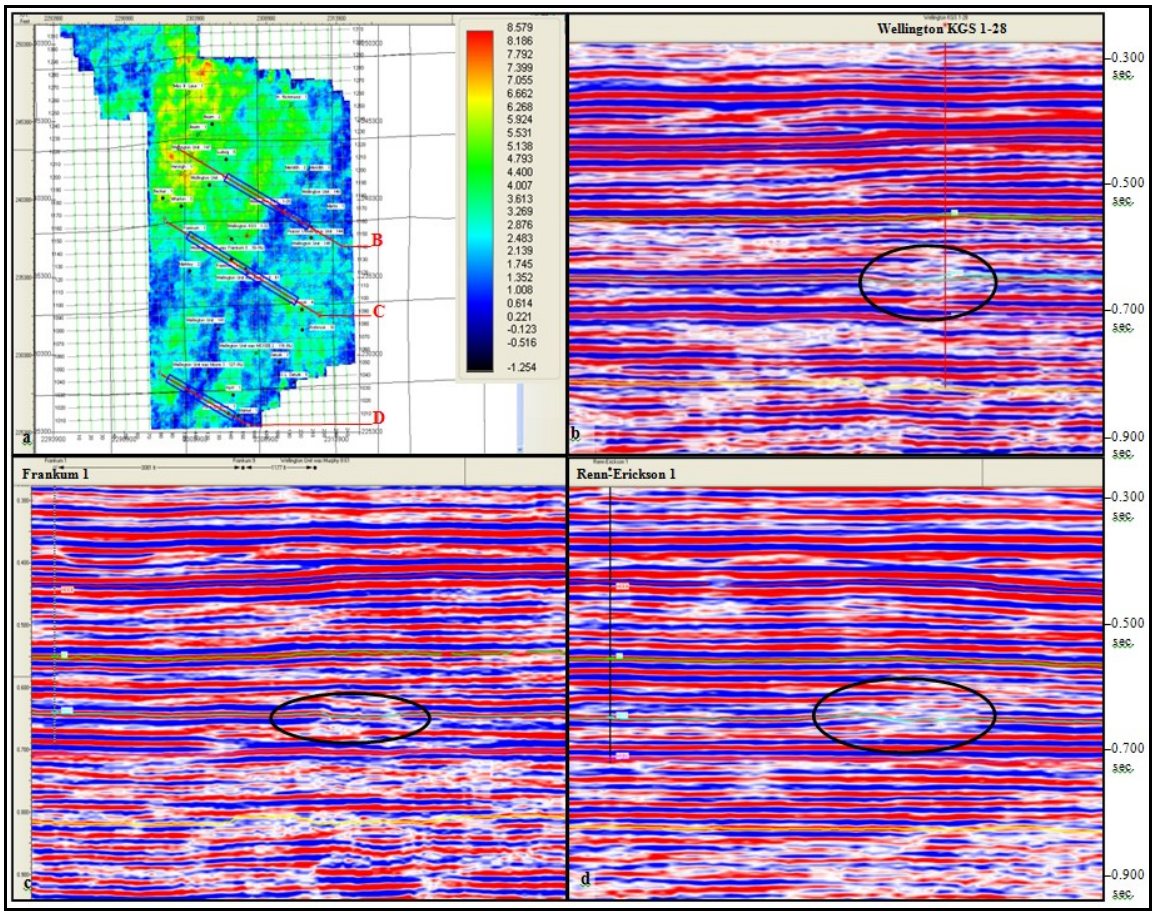

Figure 27 (a) Seismic amplitude extracted along the horizon of the Mississippian-top in the Wellington 3D seismic data set with locations of seismic cross sections shown in (b), (c) and (d) with amplitude dimming (marked with ellipses). (Ohl and Raef, 2012. Journal of Applied Geophysics, under review)

Seismic cross sections of Figure 27 b, c, and d demonstrate the amplitude dimming effect seen throughout the seismic reflection event of the Mississippian horizon. The anomaly, as seen from Figure 27 a, b, c, and d, is more of a lateral change than a vertical change in amplitude. Lateral changes in amplitude are usually associated with lateral changes in porosity (Bacon et al,. 2003). Proper understanding of these features is essential in both carbon dioxide flood management and building a sound reservoir characterization for geosequestration. Special

emphasis should be placed upon studying these smaller features, which may potentially lead to implications that govern the movement of the carbon dioxide plume.

Coherency and curvature will be discussed together, as they complement each other in the interpretation of seismic data. Both of these seismic attributes gives the interpreter insight into the structural effects on the seismic data. Within the study area, coherency and curvature strongly agree with each other that there are multiple structural features present in the seismic. Figure 28, shows an extracted seismic coherency horizon for the top of the Mississippian formation. It is important to note that the coherency features present trend in the same direction of other known faults in the area, which have been linked to the Nemaha Uplift or Mid-Continent Rift (Baars and Watney 1991). These similar trending features can be seen in Figure 28 as green arrows showing their orientation. The yellow circle seen in Figure 28 denotes a suggested location for a carbon dioxide injection site. Establishing this location as an injection site could severely impact the manner for which the carbon dioxide would migrate once injected into the formation.

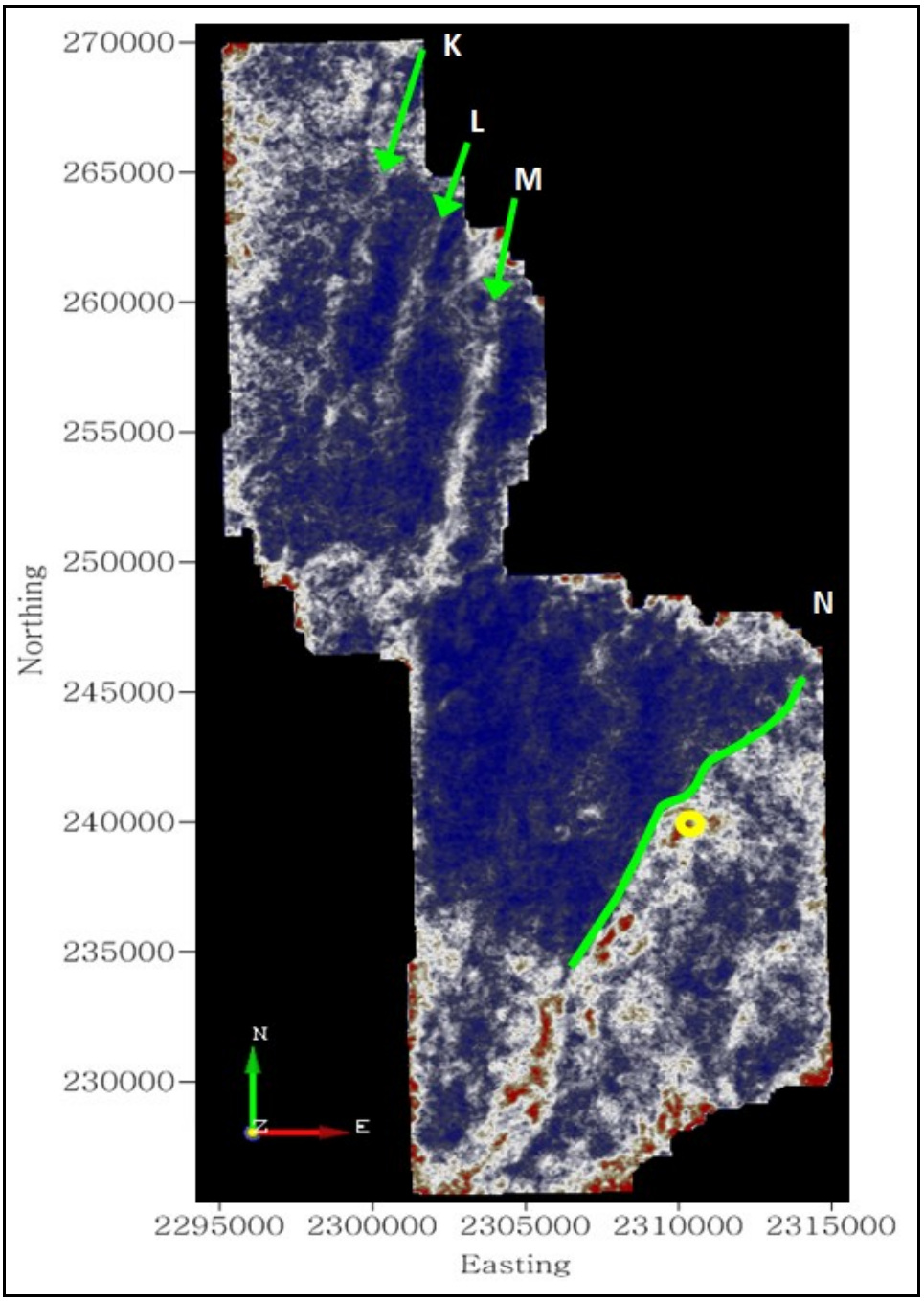

Figure 28 Coherency attribute Mississippian horizon map showing the linear anomaly trending NNE. The green arrows denote the fault/fracture orientation within the study area which correlates very well with features caused by the Nemaha Uplift as seen back in Fig. 1b; the yellow circle shows the location of a proposed CO2 injection site and the green arrows to coherency anomalies K through to N. (Ohl and Raef, 2012. Journal of Applied Geophysics, under review)

Figure 29, shows the extracted curvature horizon for the top of the Mississippian formation and all major curvature feature are in agreement with the coherency features. This helps to distinguish these features are not artifacts introduced during processing, because these two structural attributes are calculated using different seismic variables. Also, the curvature features line up with the known faults in the area that Baars and Watney (1991) refer to. This correlation of seismic structural attributes helps solidify that the features in the study area are resultant from the Nemaha Uplift.

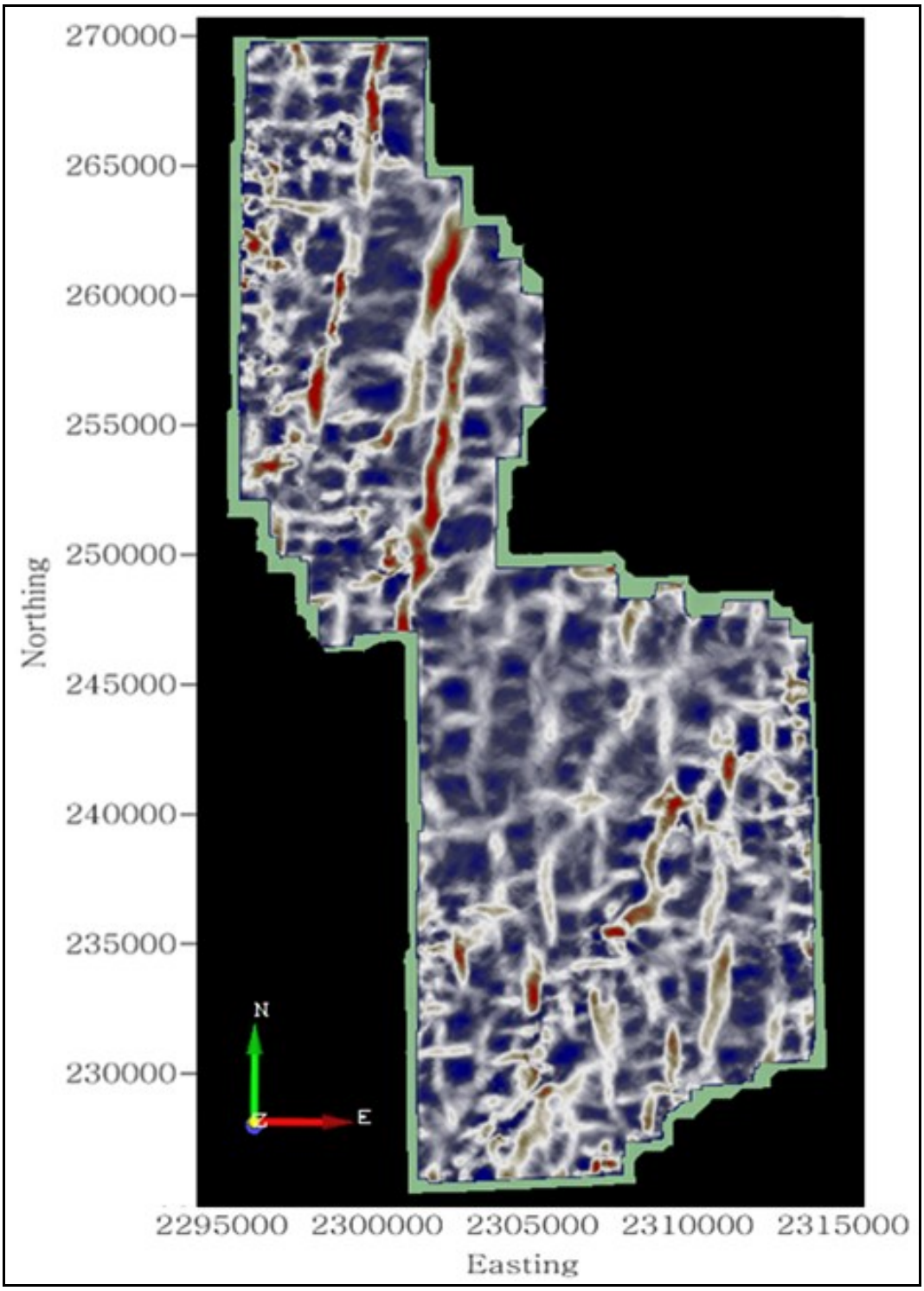

Figure 29 Most negative curvature map generated in house showing fault and fracture patterns within the seismic survey. Red areas show possible faults within the seismic survey.

Figure 30, is a most negative curvature map of the Mississippian that has been generated by Susan Nissen at Geotexture, a consulting geophysicist that is collaborating on the project. Susan's curvature and curvature ran at Kansas State University is in agreement with each other, solidifying the fault and fracture pattern within the seismic surveys.

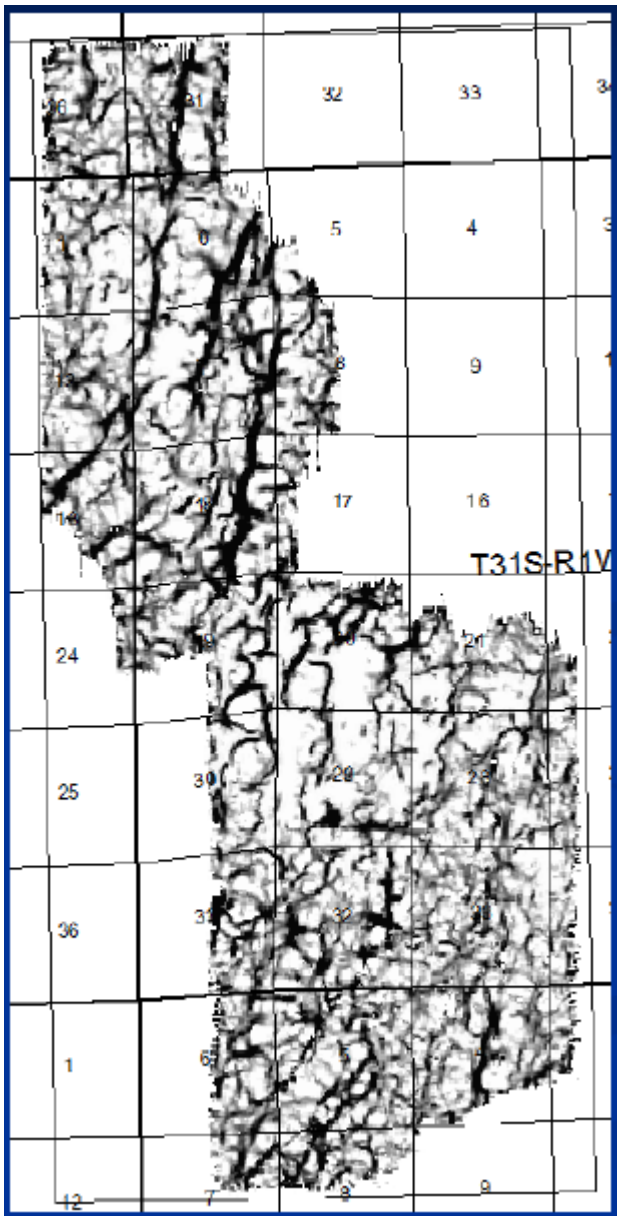

Figure 30 Most negative curvature for the study area calculated by Susan Nissen at Geotexture.

The continuity of the overlapping low coherency and dimmed amplitude anomalies, vertically (time/depth) and horizontally (aerially), is shown in Figures 27 and 28. This continuity suggests that the genesis is of a real geological cause rather than an artifact related to acquisition footprints or inadequate processing. The trend (NNW-SSW) of the linear coherency and amplitude dimming anomalies is in agreement with regional trend of the midcontinent rift system. The midcontinent rift system is a NNW-SSW trending fault zone affecting the Precambrian basement that was reactivated during the Paleozoic (Baars and Watney, 1991). A new well (Wellington-KGS 1-28) was drilled targeting the easternmost amplitude anomaly; a reworked lithofacies was revealed that is strongly suggestive of structural control on lithofacies. This reworking of the subsurface also evidence of a compound contribution of structural elements imprinted by reworking of lithofacies along possibly spatial extension of basement faults due to reactivation.

The artificial neural network portion of the study resulted in results that were greater than expected. Two neural networks were applied to the Mississippian formation for further validation in the process. Porosity variation has been determined from the results of the neural networks to play a major role in certain coherency and amplitude anomalies seen in the seismic data.

In preparation of training a supervised artificial neural network for distinguishing different classes of petrophysical facies, we examined a cross-plot of average well log neutron-porosities against the Mississippian horizon amplitude (Figure 31), for several wells within our study area. Porosity values greater than twelve percent are considered class one, class two porosities are between eight and twelve percent, while class three porosities are values lower than eight percent. The three petrophysical “lithofacies” classes, as exemplified by a 3D cross-

plot (Figure 32), of a sub-volume of the three attributes used in the training of the ANN manifest clear separation. It is evident that the seismic attribute set used in the cross plot and in the ANN training provides acceptable discriminatory "space" for petrophysical/lithofacies classification in the study area. Class one (higher porosity) had higher values for the three calculated attributes. Class two (middle porosity) had the lowest values for the calculated attributes. Class three (lowest porosity) had high bandwidth measurement while having low energy and peakedness values.

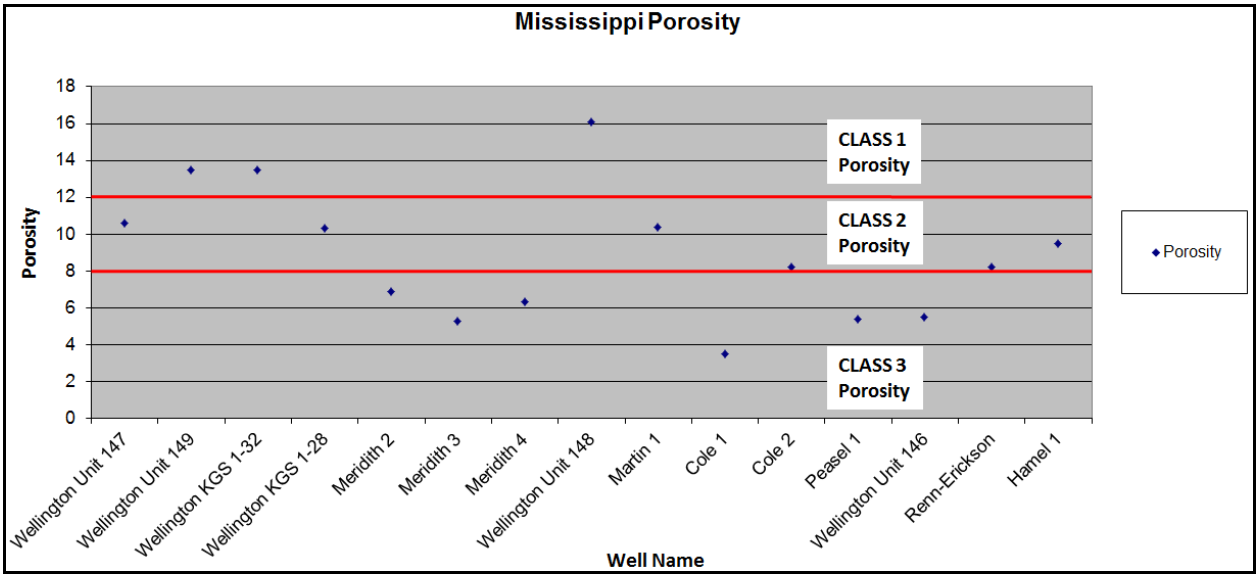

Figure 31 Showing the Mississippian porosity values for wells throughout the survey broken into their respected petrophysical facies classes to be used in the neural network.

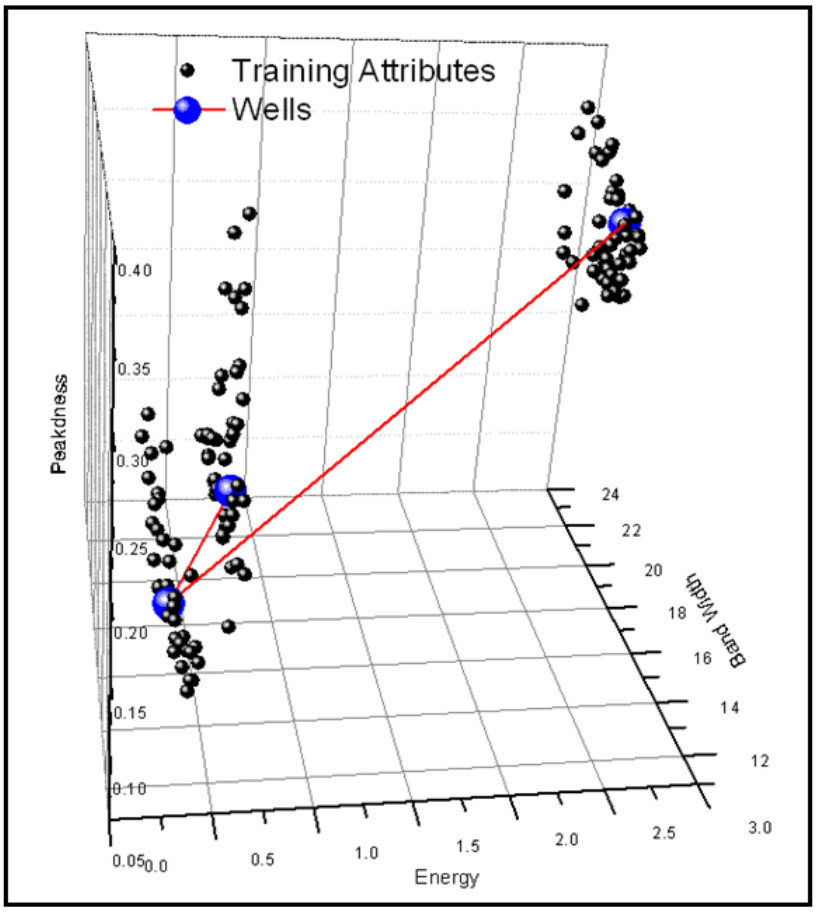

Figure 32 Class-type wells in the selected attributes cross-plot space that was used to train the neural network. (Ohl and Raef, 2012. Journal of Applied Geophysics, under review)

After successful training of the network, a performance test was ran to see how well the network would classify the porosities with the seismic attributes. Figure 33, shows the improvement over multiple iterations as mean squared error for training, validation and test subsets. The low mean squared error value of our trained network is indicative of the high potential of successful application to the classification of the seismic waveform of the Mississippian horizon.

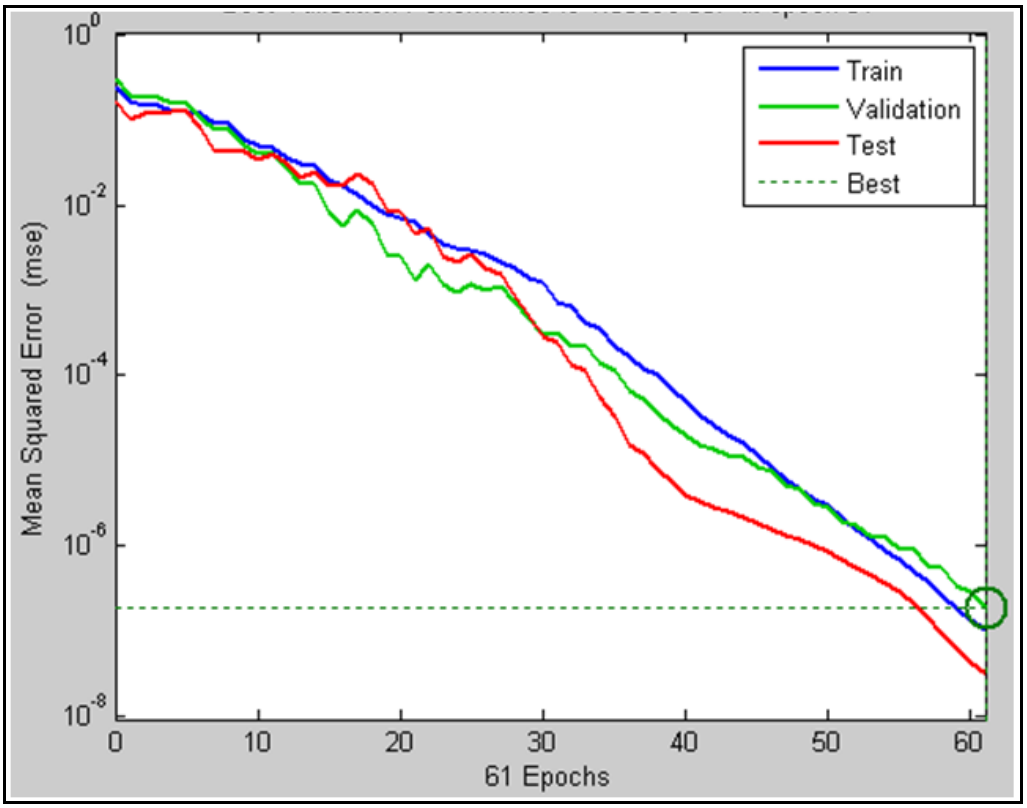

Figure 33 Performance test in mean squared error with iterations "epochs" of the training, validation, and applied LVQ network. (Ohl and Raef, 2012. Journal of Applied Geophysics, under review)

After running the performance test, we then ran our seismic survey through the neural network, which resulted in a petrophysical facies classification map (Figure 34). In Figure 35, we overlay the coherency lineaments "faults" K through N on the petrophysical/lithofacies classification map of Figure 34 with the aim of illustrating different relational aspects and controls of the faults on petrophysical/lithofacies variation. Future CO_2 injection monitoring is likely to shed more light into the role of lineaments/faults that have to be taken into account for both carbon geosequestration and CO_2 enhanced oil recovery plans. It is of importance to point out that the northeast part of the southern survey has a lithofacies contact, between class one and class three facies types, that is in clear coincidence in position with the

NE part of lineament N; amplitude anomaly location is marked with solid line. This coincidence points to higher probability of structural control on facies distribution; the same situation is valid for lineament L.

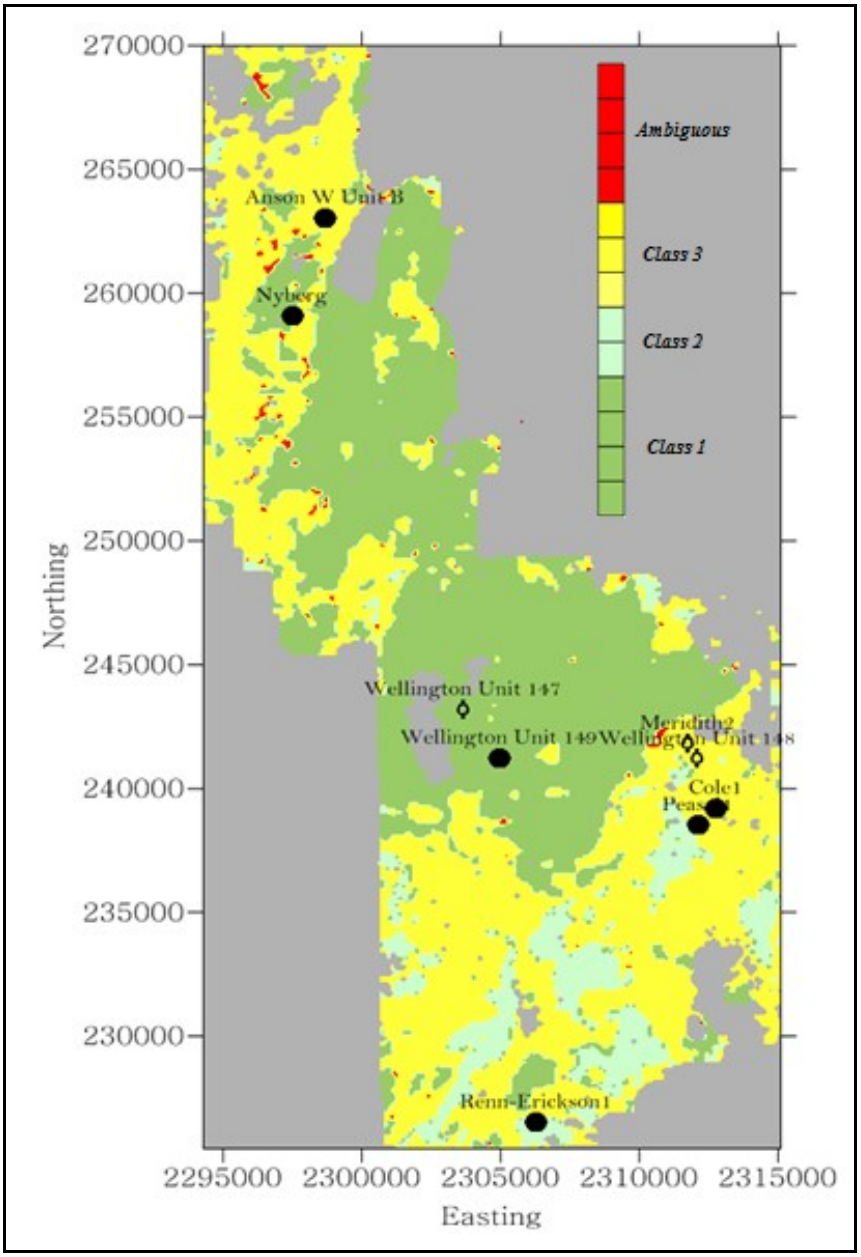

Figure 34 Seismic (petrophysical/lithological) facies map of the Mississippian based on the application of the trained competitive neural network. (Ohl and Raef, 2012. Journal of Applied Geophysics, under review)

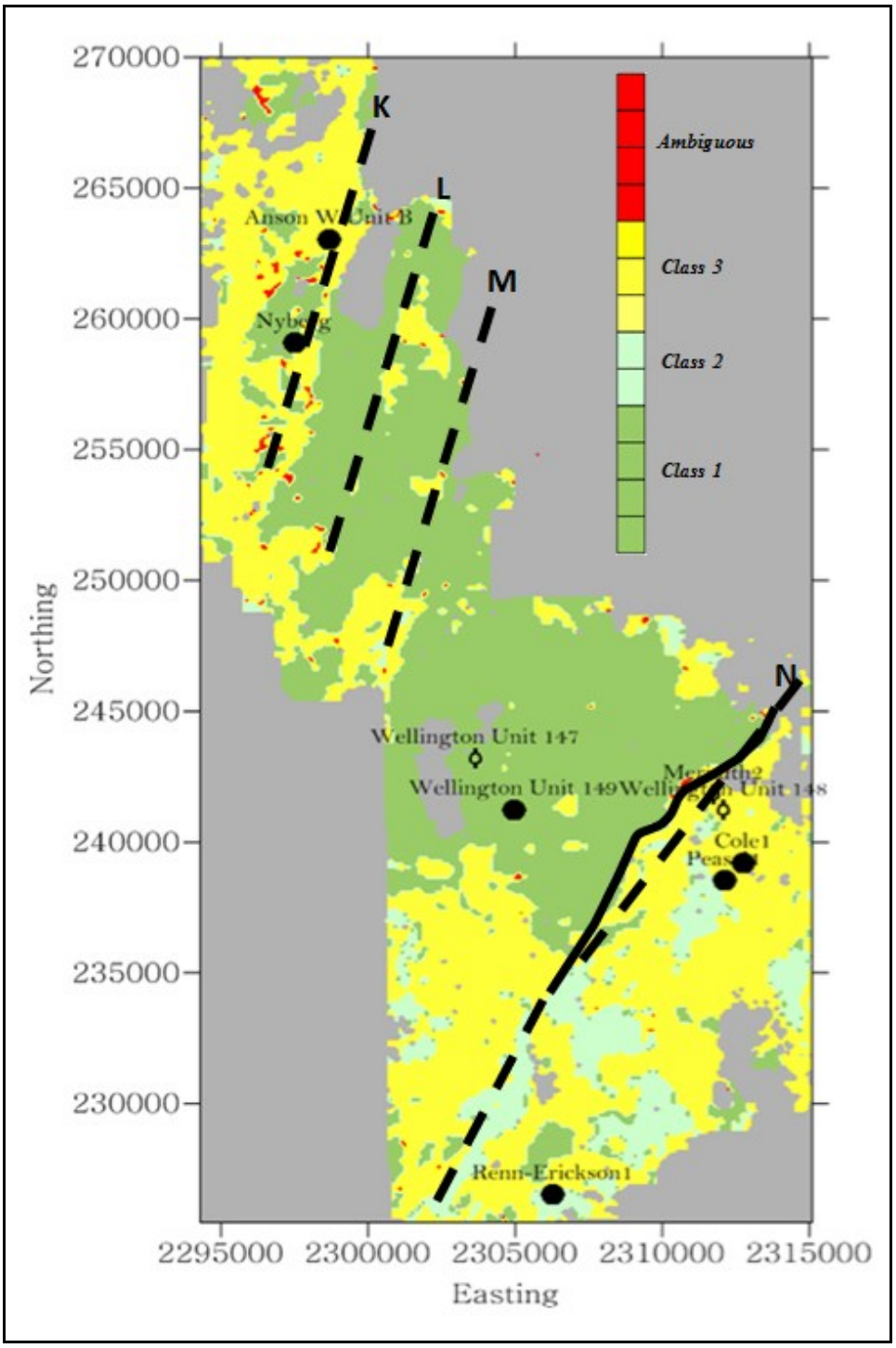

Figure 35 Seismic (petrophysical/lithological) facies map of the Mississippian with the coherency lineaments overlaid as dashed lines; the solid line indicate location of amplitude anomaly where it deviates from the corresponding lineament "N" of Figure 28. (Ohl and Raef, 2012. Journal of Applied Geophysics, under review)

In Figure 36, a cross-plot of neutron porosity against acoustic impedance –color-coded to match classes in Figure 35. Cross-plot includes three wells which were not included in the neural network training, but corroborate with the results of the artificial neural network petrophysical/lithofacies relevance to reservoir petrophysical properties.

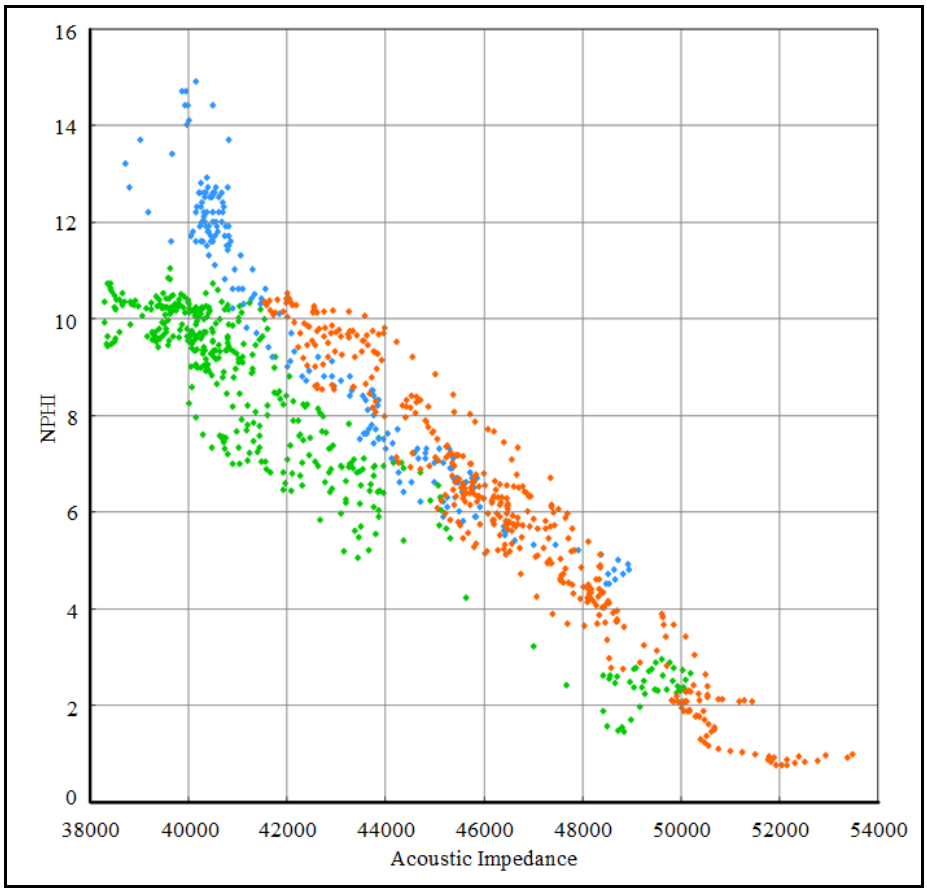

Figure 36 Cross-plot of well log porosity against acoustic impedance of the Mississippian indicating separable clustering based on acoustic impedance, at three not-selected in training the ANN, wells, thus relevance of seismic wavelet characteristics (bandwidth, energy, and peakedness) to petrophysical facies classification for the Mississippian depleting reservoir. The wells used in this cross-plot were color coded so as to correspond to their petrophysical class color as seen in Figure 35. (Ohl and Raef, 2012. Journal of Applied Geophysics, under review)

A secondary neural network, done in OpendTect, was ran for the seismic data, using different wells than the first neural network ran in Matlab. The results from the two different neural networks are very similar, giving confidence in the use of the neural network to help characterize petrophysical facies within the study area. It is also important to note the OpendTect neural network used the same seismic attributes as input layers, but different wells were used to restrain the correlation and yielded almost the exactly same petrophysical facies map, as seen in Figure 37.

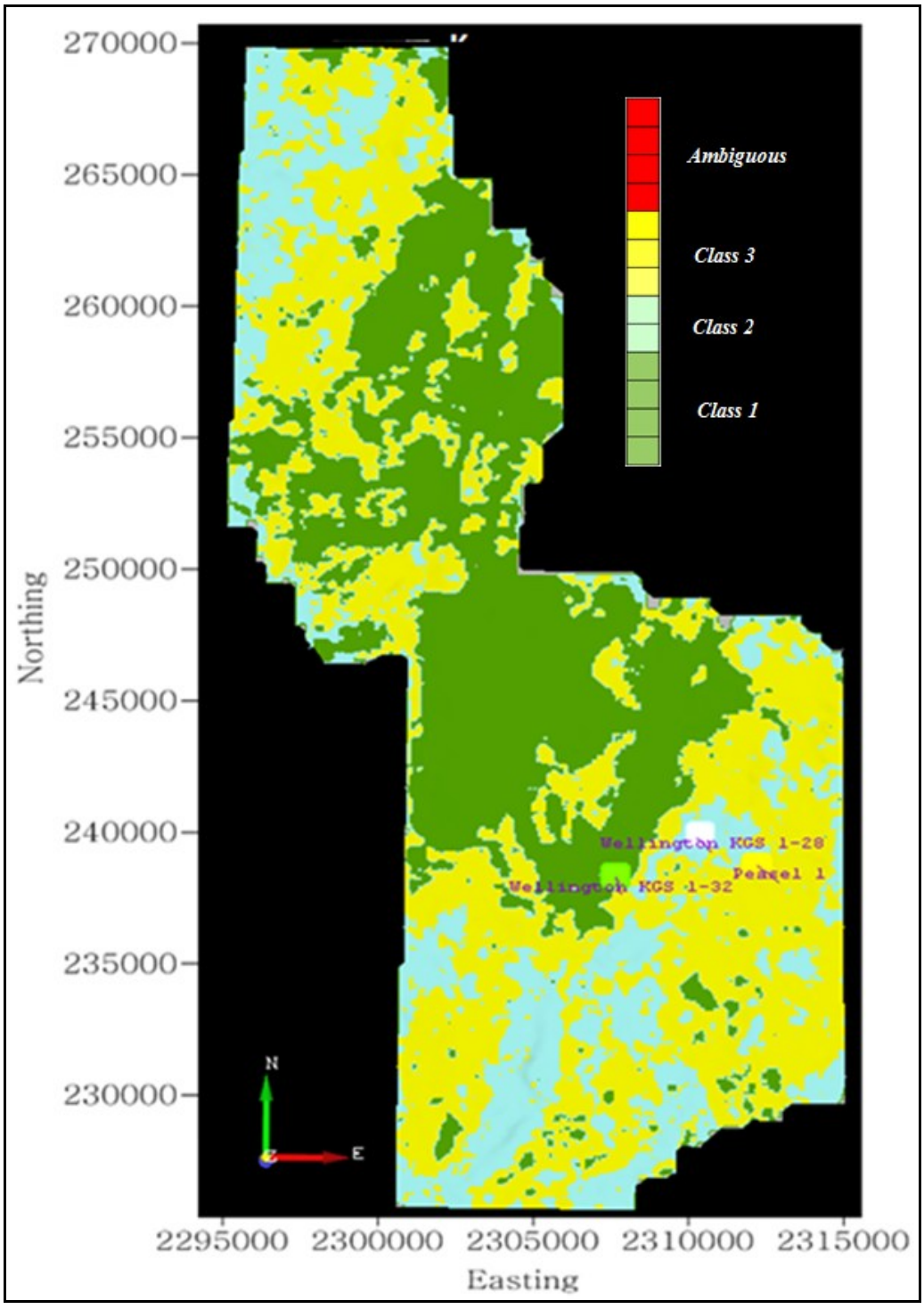

Figure 37 Shows the OpendTect neural network petrophysical facies map for the top fifty feet of the Mississippian formation. High porosity values are seen in green, moderate porosity values are in blue, while low porosity values are yellow.

Training of the OpendTect neural network was of high success (Figure 38) with misclassification of the seismic data approximately or less than five percent. This high quality classification of the seismic data, by the neural network, is significant and allows the interpretation of the neural network to be used in the overall interpretation of the rock formations. Further validation of the OpendTect neural network, by adding several other wells, shows a good correlation between the neural network petrophysical facies map and the well log porosities. Figure 39, shows the petrophysical facies classes map with multiple wells in their respected petrophysical facies class. All wells that were added for validation, after obtaining the petrophysical facies map, fell into their appropriate classes. This helps show the successful training and application of the neural network to the seismic data.

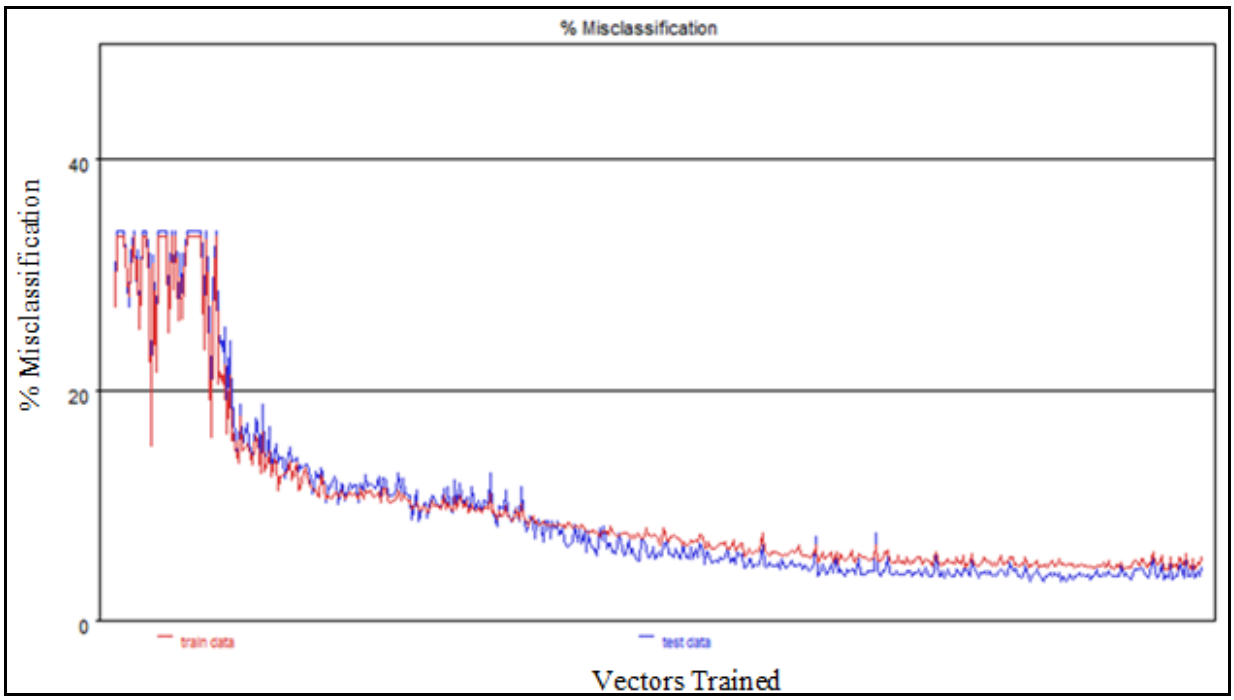

Figure 38 Misclassification of the seismic data by the neural network. The misclassification was at, or below, five percent, resulting in a high quality correlation between the seismic data and the neural network. Test data is blue in color while train data is red in color.

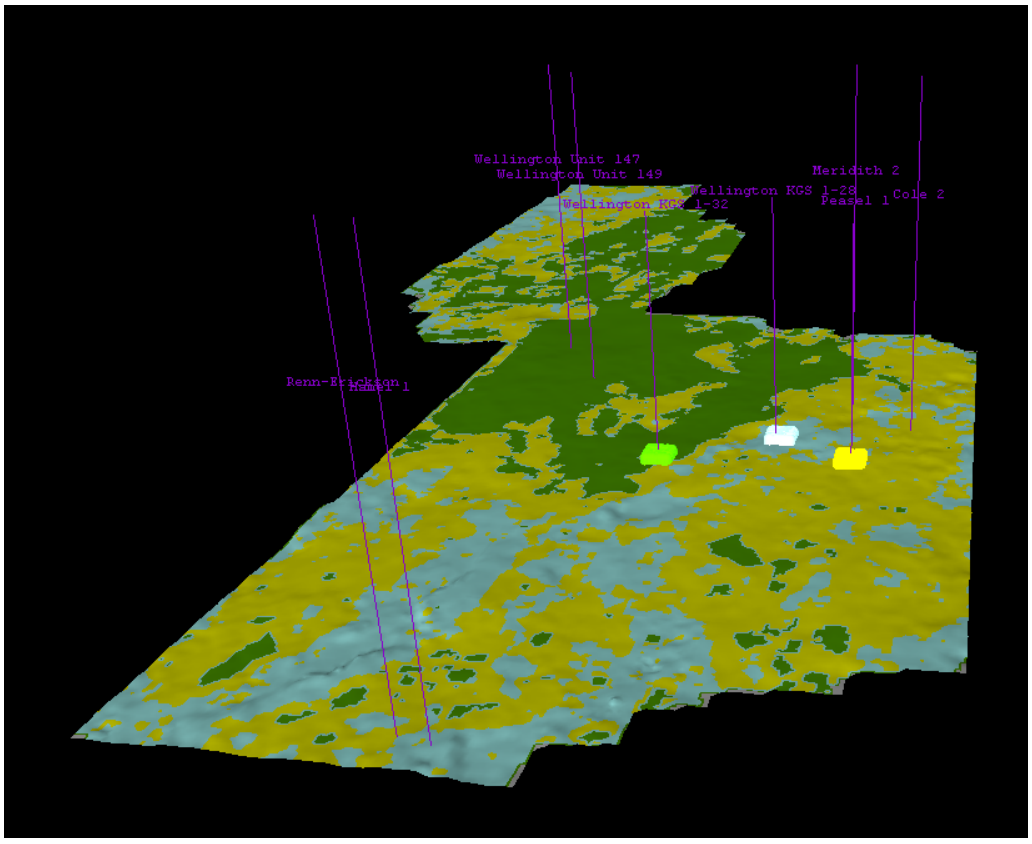

Figure 39 Shows multiple wells for each petrophysical facies class falling within their respected classes giving further validation that the process was successful in its training and application of the neural network.

Based on the previously discussed results for the Mississippian formation, it is clear that both structural features and petrophysical features are of interest. Faults within the study area are most likely associated with the Nemaha Uplift and further reworking of certain faults has resulted in porosity changes that effected and caused amplitude anomalies. The fault and fracture pattern for the study area is mostly North Northeast trending, with smaller fractures occurring perpendicular to the major lineaments. This fault and fracture analysis is key information that will need to be input into the reservoir model of the Department of Energy project to better model the sequestration of carbon dioxide in the Mississippian depleted hydrocarbon reservoir.

Arbuckle Characterization

Arbuckle penetration in the area being very limited makes it more difficult to correlate well properties to seismic attributes. Only four wells within the study area have penetrated the Arbuckle and have geophysical well logs ran through the formation. The formation top has been generated along with amplitude slices, which do not show any features as alarming as the Mississippi feature. With the addition of the two wells that the KGS just completed drilling, Arbuckle characterization will be assisted by, up to date logs.

Arbuckle amplitude does not show any features as disturbing as the Mississippian feature but the Arbuckle amplitude does show signs of faulting within the Anson-Bates portion of the survey. These faults can be seen on the seismic amplitude map of the Arbuckle in Figure 40. Three amplitude features in the Anson-Bates portion of the survey demonstrate characteristics of faults in the seismic amplitude horizon slice. They show up as lineaments with drastic change in amplitude. These features, if they are faults, are located closer to the Precambrian basement and therefore have a greater chance of being effects from the Nemaha Uplift events. It is important to note that the main anomalous feature seen in the Mississippian formation does not extend down into the Arbuckle formation; however, lineaments in the Anson-Bates area are visible in both formations.

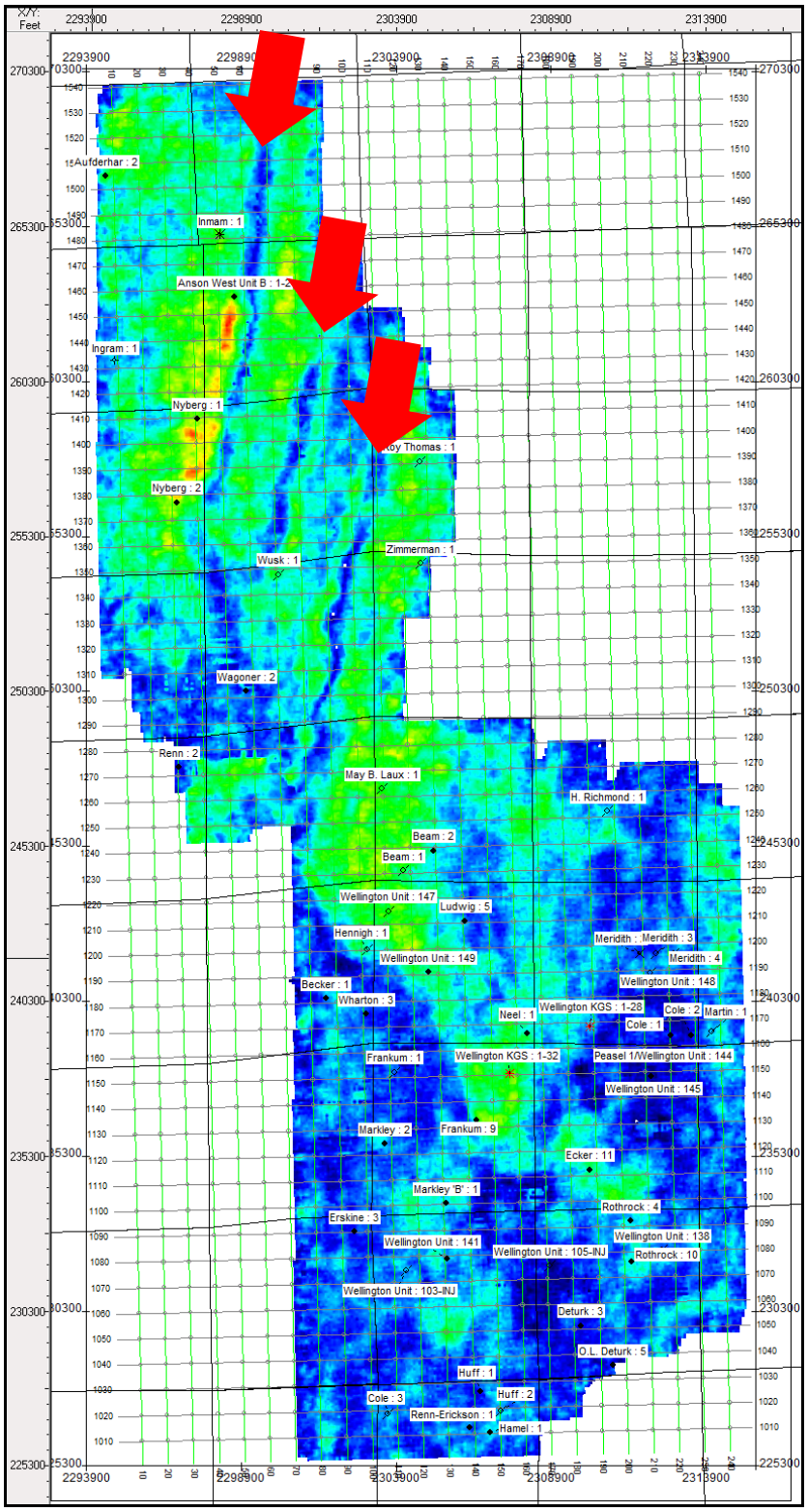

Figure 40 Arbuckle amplitude map demonstrating amplitude anomalies in the upper Arbuckle formation. Red arrows show possible faulting seen in the amplitude map.

Arbuckle coherency allows us to further interpret features seen in the Arbuckle amplitude map. Figure 41, map of Arbuckle coherency showing lineaments in the northern half of the seismic data that could be interpreted as faults. As discussed in the Arbuckle amplitude results section, these lineaments are very similar to lineaments seen in the Mississippian formation, which strongly helps interpret them as faults. The characteristics of the lineaments are also in agreement with other seismic interpreted faults in several academic papers and books. Figure 42, is a seismic cross-section showing the major fault from the Anson-Bates survey.

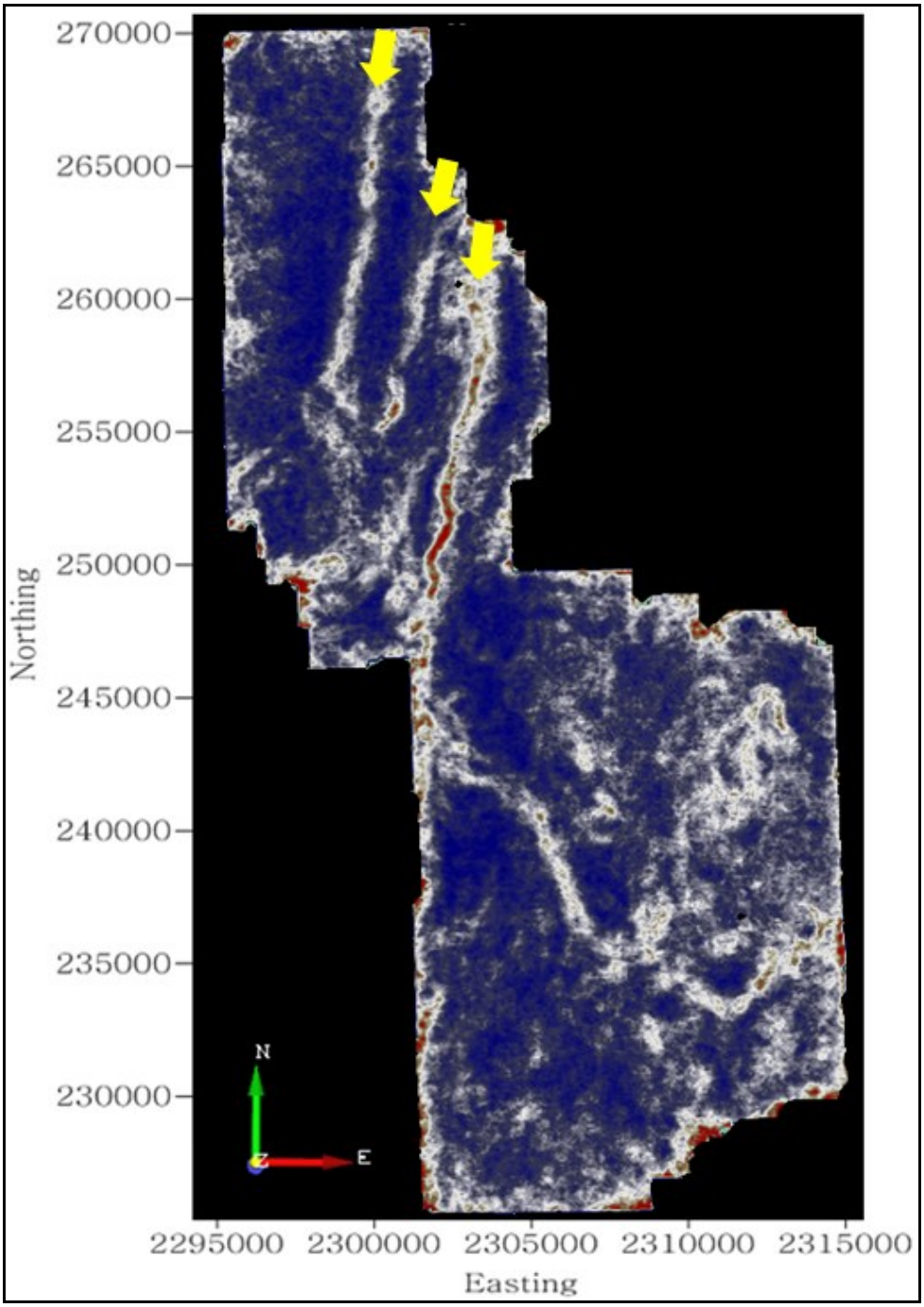

Figure 41 Arbuckle coherency map showing faults in the Anson-Bates portion of the survey. Yellow arrows show very similar lineaments as seen in Figure 40. This lineaments are interpreted as faults.

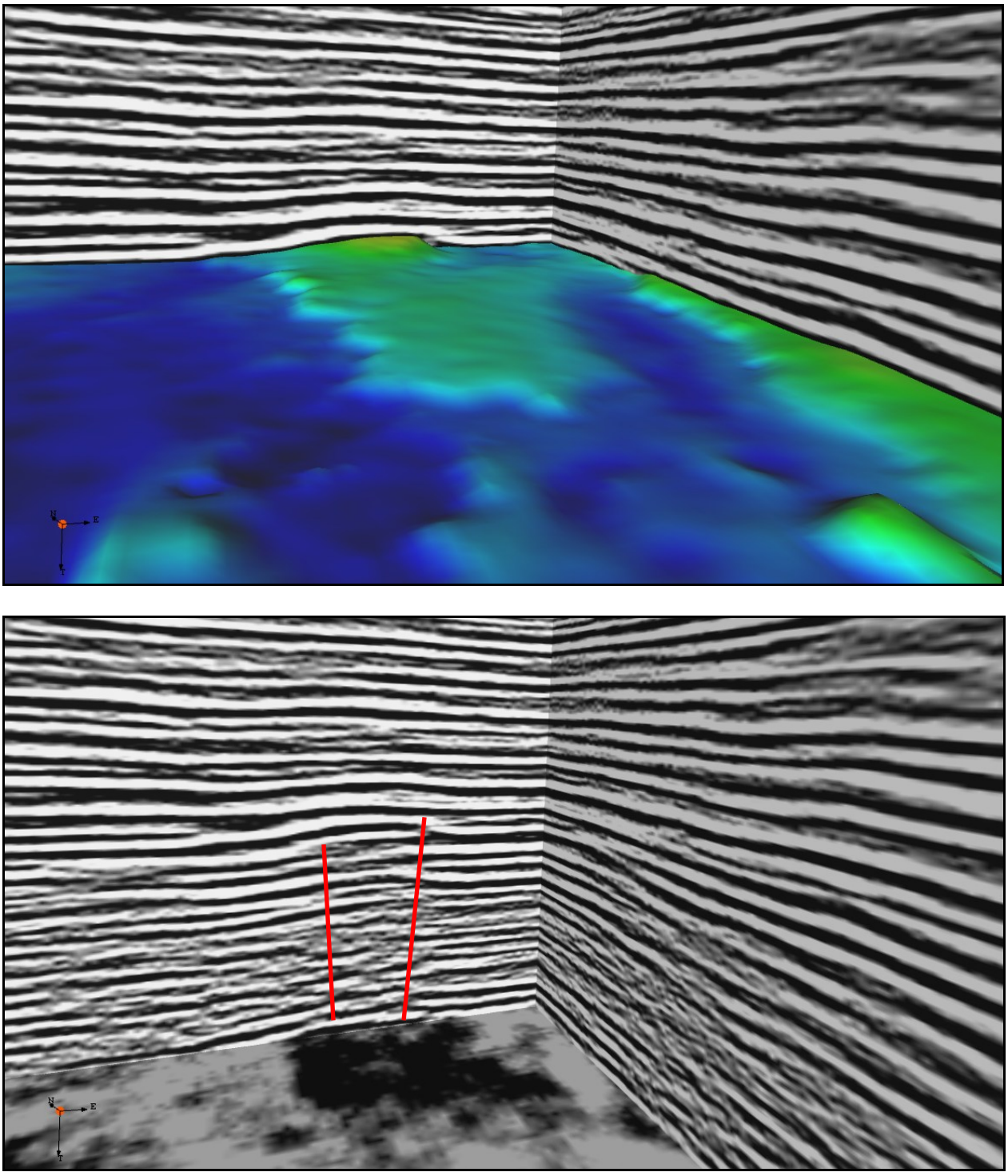

Figure 42 Seismic cross-section showing interpreted faults (red lines) in the Anson-Bates survey that was donated by Nobel Energy.

The Arbuckle curvature attribute also aided in the interpretation of the structural features seen in the Arbuckle amplitude map. Curvature is sensitive to dipping of the rocks and is a great tool for seeing faults and fractures within the formation due to minute changes in the rocks. The northern three amplitude and coherency features also show up on the curvature for the top of the Arbuckle, (Figure 43) and therefore allow interpretation of faults. Curvature is also an important seismic attribute for determining the fault and fracture orientation within the survey. Figure 43 shows that the fault and fracture pattern is similar to the Mississippian, trending North Northeast. Once again, this fault and fracture orientation is in agreement with the orientation associated with the Nemaha Uplift, and therefore strengthens our conclusion that these features are results from the Nemaha Uplift event.

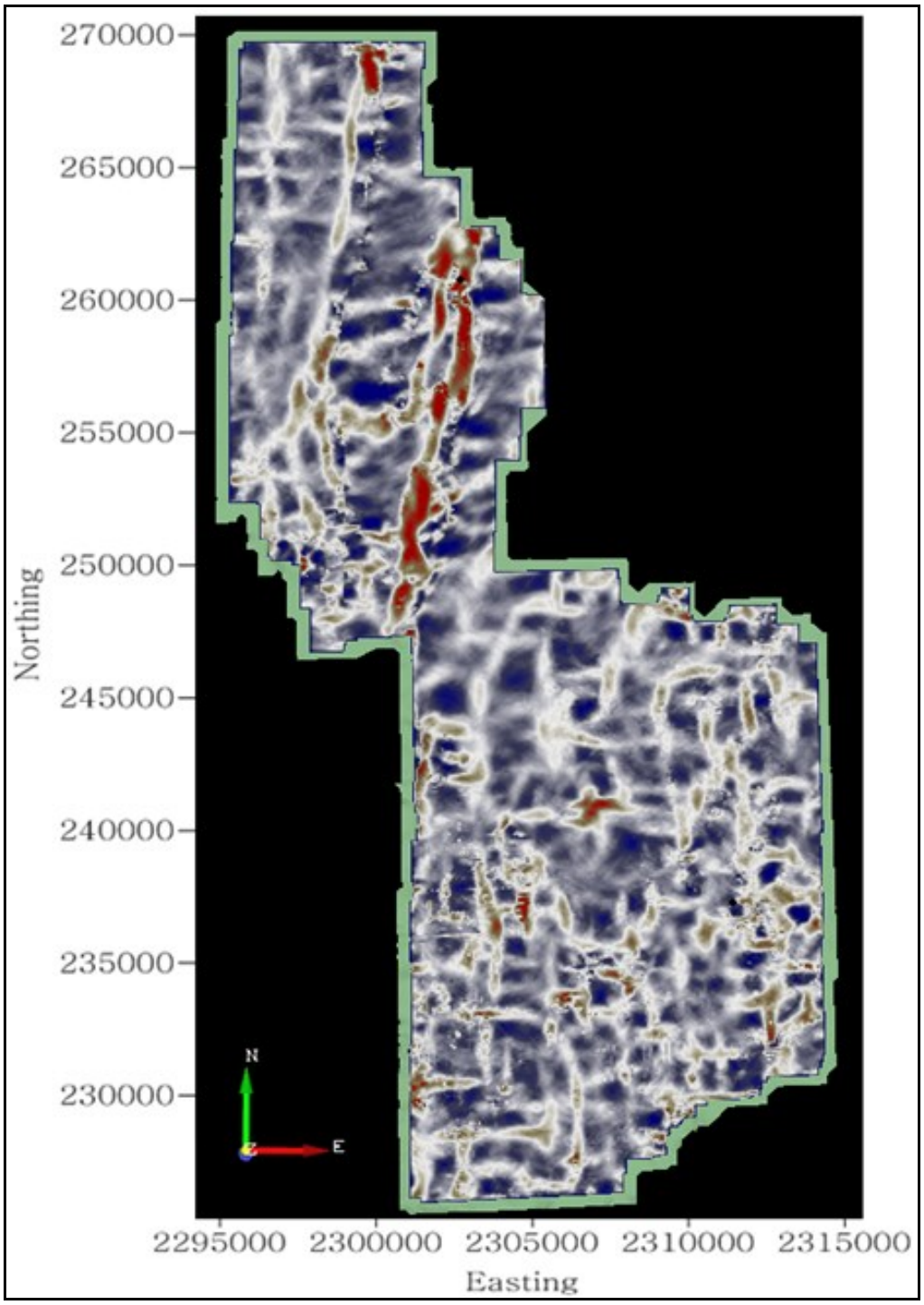

Figure 43 Arbuckle curvature showing similar results as the coherency. Faulting is present in the Anson-Bates portion of the survey. Curvature also shows the fault and fracture pattern for the upper Portion of the Arbuckle formation. The trend of the fault and fracture pattern is in agreement with the Nemaha Uplift trend.

Just like the Mississippian, an artificial neural network was trained and applied to the Arbuckle horizon. The Mississippian parameters were utilized, and for the most part, kept the same for the Arbuckle neural network. The same three seismic waveform attributes: energy, peakedness, and bandwidth were used to train the neural network in order to classify the Arbuckle horizon. The only difference between the OpendTect Mississippian neural network and the Arbuckle neural network was a change in wells used to train the network. The Arbuckle used the Renn-Erickson well instead of the Peasel 1 well. This change in wells was because of well log porosities for each well. Figure 44, shows the well log porosities for wells that penetrate far enough into the Arbuckle formation. Porosity classes were similar to that of the Mississippian, but change in class was noticed for most wells. Porosity classes in the Arbuckle were as follows: class one porosities were twelve percent or higher, class two porosities were twelve to eight percent, and class three porosities were lower than eight percent.

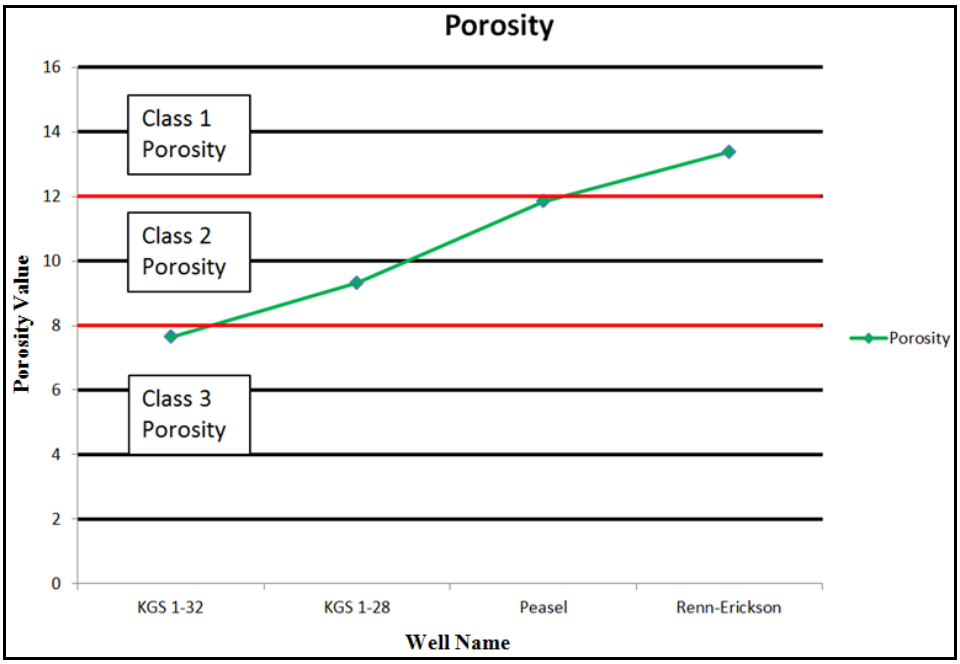

Figure 44 Average Arbuckle porosities for wells, which penetrate the Arbuckle formation far enough, that helped train the neural network to characterize the Arbuckle horizon in terms of petrophysical facies.

These petrophysical facies utilizing well logs allows the neural network to apply changes in the seismic waveform to changes in porosity from well logs and application of the neural network on the seismic data yields a petrophysical facies map. Figure 45, is the petrophysical facies map for the Arbuckle formation.

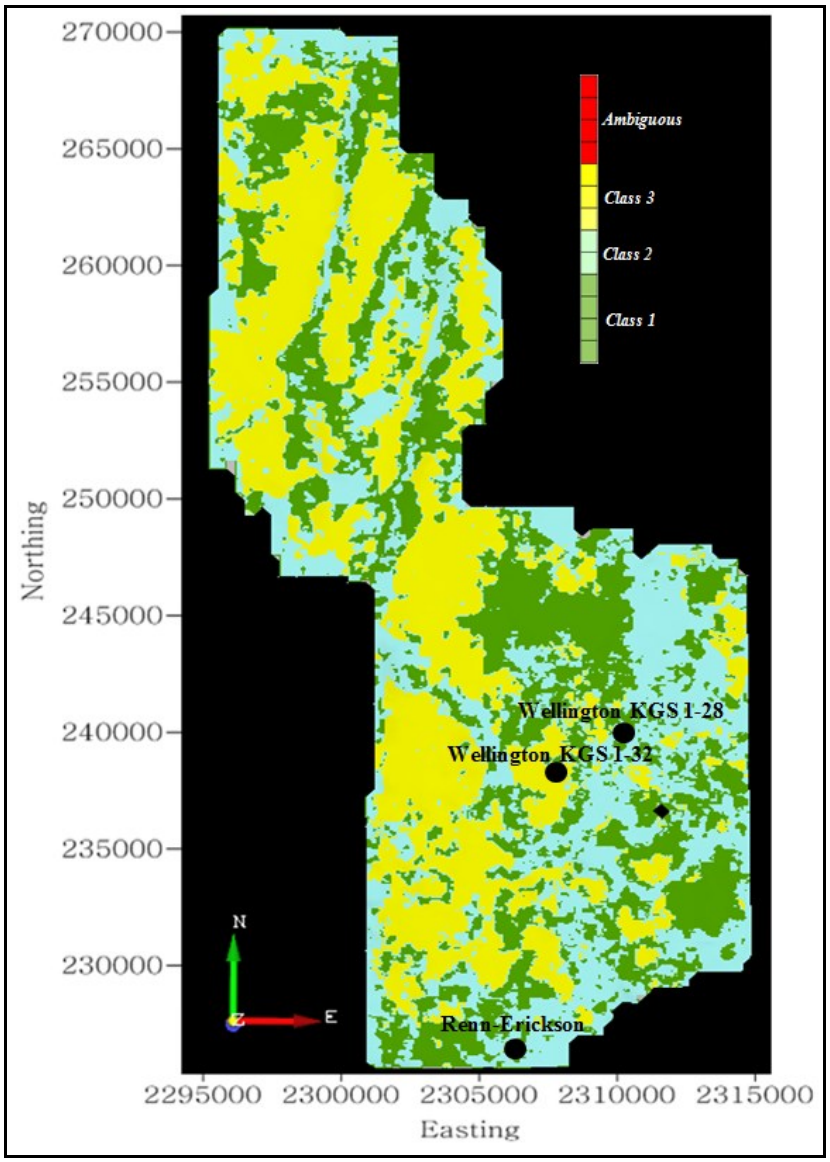

Figure 45 Petrophysical facies map of the Arbuckle horizon. High porosity values are seen in green, moderate porosity values are in blue, while low porosity values are yellow.

Training of the OpendTect neural network was of high success (Figure 46) with misclassification of the seismic data at approximately ten percent. This high quality classification of the seismic data, by the neural network is significant and allows the interpretation of the neural network to be used in the overall interpretation of the rock formations. The Arbuckle has a greater misclassification percentage than the Mississippian, because of the strength of the reflector associated with the two horizons. The Arbuckle is deeper than the Mississippian and as seismic energy travels further into the earth its strength is decreased by attenuation, reflection, absorption, etc. This decrease in the strength means the strength of the energy recorded will be less and therefore recording lower amplitudes. Lower amplitude reflections in seismic data make correlation, picking, and interpretation more difficult. Because of these factors the Arbuckle neural network had a harder time with training and application to the seismic data.

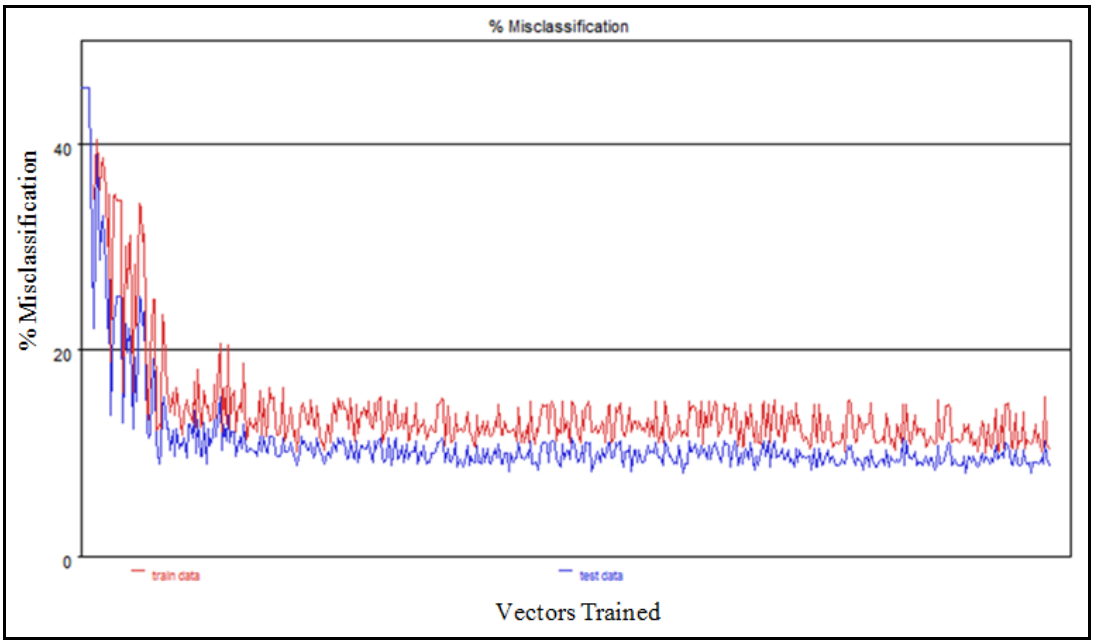

Figure 46 Arbuckle neural network misclassification chart showing average misclassification of the Arbuckle horizon at 10 percent. Test data is blue in color while train data is red in color.

Chapter 5 - Conclusion

Carbon geosequestration plans in southern Kansas will greatly benefit from integrating multi-scale datasets –geophysical well logs, 3D seismic reflection data, regional basement tectonic faults, and depositional and stratigraphic frameworks– in pursuing sound rock formation characterization and robust static and dynamic subsurface models. Understanding and building discriminatory workflows for small-scale structural and/or litho-stratigraphic features are of paramount importance. These features can improve the building of up-to-date reservoir models, which are essential to successful flow simulation of carbon dioxide plumes. Understanding these flow simulations will provide insight to planning a successful carbon dioxide based enhanced oil recovery or geosequestration application.

In this case study, seismic waveform attributes of the Wellington and Anson Bates Mississippian and Arbuckle horizon along with neutron log porosities in an artificial neural network training that was applied to the entire seismic survey yielded a petrophysical/lithofacies classification map. This classification has been corroborated using cross plots of the used attributes space and of acoustic impedance against neutron log porosities of three wells, which were not included in the training.

Incorporating the litho/petrophysical facies map along with the coherency and amplitude attributes, it is most likely that the anomalous features seen within the Mississippian are old fault systems associated with the Nemaha Uplift that since activation has gone through a reworking process. This reworking process has caused the petrophysical properties of the formation rocks to register different on multiple well log instruments.

The major Mississippian amplitude dimming anomaly not being present in the Arbuckle, is most likely due to the different unconformities and the time gaps associated with deposition. The lineaments in the Anson-Bates survey, however, are present in both formations suggesting that these faults are post Mississippian deposition. This faulting time frame supports the hypothesis that a reactivation fault or fracture towards the top of the Mississippian formation has undergone reworking or erosion, resulting in the amplitude dimming anomaly seen in the seismic data. This porosity change could cause problems if one was to undergo a carbon dioxide enhanced oil recovery flood within the Mississippian producing formation.

The Arbuckle, on the other hand, did not possess any large amplitude dimming anomalies. However, the Arbuckle does have three major faults in the northern half of the seismic survey that was detectable by seismic amplitude, coherency, and most negative curvature. These faults need to be further evaluated to see if they are trapping faults or if these faults would provide a migration highway for supercritical carbon dioxide to travel along. If these faults would provide a migration pathway for carbon dioxide to travel along then someone must look into the seal integrity of the overlying rocks in order to see if the plume would be stopped from rising to the local ground water or even worse, the surface. It is also important to make sure that these fault and fracture patterns make it into the reservoir model in order to see how they will affect the migration of the carbon dioxide after sequestration.

Further research, which could be done to help support this work, would include: 1. Seismic inversion, which would allow for further characterization of the change in porosity. 2. Seal integrity work looking into seismic characterization of shale beds within the survey. 3. Further analysis of the neural networks, incorporating more seismic attributes to potentially give a more accurate representation of the changes in porosity within the formations spatially.

References

Arts, R., Eiken, O., Chadwick, A., Zweigel, P., Van der Meer, L., and Zinszner, B., 2004. Monitoring of CO2 injected at Sleipner using time-lapse seismic data. Energy. 29, 1383-1392.

Arts, R.J., Elsayed, R., Eiken, O., Chadwick, A., Kirby, G., Ostmo, S., Zinszner, B., and Meer, L.V.D., 2002. Estimation of the mass of injected CO2 at Sleipner using time-lapse seismic data. European Association of Geoscientists & Engineers. Expanded Abstracts, H016.

Baars, D.L. and Watney, W.L., 1991. Paleotectonic control of reservoir facies. Kansas Geological Survey. Bulletin 233, 253-262.

Bachu S., 2003. Screening and ranking of sedimentary basins for sequestration of CO2 in geologic media in response to climate change. Environmental Geology. 44, 277-289.

Bacon, M., Simm, R., and Redshaw, T., 2003. 3-D Seismic Interpretation. Cambridge, United Kingdom.

Bahorich, M. and Farmer, S., 1995. 3-D seismic discontinuity for faults and stratigraphic features: The coherence cube. The Leading Edge. 14, 1053-1058.

Basbug, B., Gumrah, R., and Oz, B., 2005. Simulating the effects of deep saline aquifer properties on CO2 sequestration. 56th Annual Technical Meeting, Petroleum Society.

Bickle, M. J., 2009. Geological carbon storage. Natural Geoscience. 2, 815-818

Carr, T., Merriam, D.F., and Bartley, J.D., 2005. Use of relational databases to evaluate regional petroleum accumulation, groundwater flow, and CO2 sequestration in Kansas. American Association of Petroleum Geologists Bulletin. 89, 1670-1627

Chopra, S. and Marfurt, K.J., 2007. Seismic attributes for prospect identification and reservoir characterization. SEG Geophysical Developments Series No. 11.

Chopra, S. and Marfurt, K.J., 2008. Seismic attributes for stratigraphic feature characterization. 78th Annual International Meeting, Society of Exploration Geophysicists. Technical Program Expanded Abstracts, 1590-1594.

Cortis, A., Oldenburg, C.M., and Benson, S.M., 2008. The role of optimality in characterizing CO2 seepage from geologic carbon sequestration sites. International Journal of Greenhouse Gas Control. 2. 4. 640-652.

Damen, K., A. Faaij, F. van Bergen, J. Gale, and E. Lysen, 2005, Identification of early opportunities for CO2 sequestration—worldwide screening for CO2-EOR and CO2-ECBM projects: Energy, 30, 1931-1952.

Doughty, C., B. Freifeld, and R. Trautz, June 2008, Site characterization for CO2 geologic storage and vice versa: the Frio brine pilot, Texas, USA as a case study: Environmental Geology, 54, 1635-1656.

Dyer, S. and Farouq Ali, S.M., 1991. Mechanistic aspects and chemistry of immiscible carbon dioxide flooding. 86th American Institute of Chemical Engineers Symposium Series, 44-51.

Friedmann, S.J., 2007. Geological carbon dioxide sequestration. Elements Magazine. 3, 179-184.

Gunter, W.D., Bachu, S., and Benson, S., 2004. The role of hydrogeological and geochemical trapping in sedimentary basins for secure geological storage of carbon dioxide. Geological Storage of Carbon Dioxide, Geological Society Special Publications, 233, 129-145.

Harilal, and Biswal, S.K., 2010. Pitfalls in seismic amplitude interpretation: Lessons from Oligocene channel sandstones. The Leading Edge. 29, 384-390.

Henry, S., 2000. Pitfalls in synthetics. The Leading Edge. 19. 604.

Hilterman, F.J., 2001. Seismic Amplitude Interpretation. 2001 Distinguished Instructor Short Course, Distinguished Instructor Series, No. 4.

Holtz, M.H., Nance, P.K., and Finley, R.J., 2001. Reduction of greenhouse gas emissions through CO2 EOR in Texas. Environmental Geosciences. 8, 187-199.

Jorgensen, D.G., 1989. Paleohydrology of the Anadarko Basin, Central United States. Oklahoma Geological Survey. Circular 90.

Kalkomey, C., 1997. Potential risk when using seismic attributes as predictors of reservoir properties. The Leading Edge. March 1997, 247-251.

Kazemeini, S.H., Juhlin, C., Zinck-Jorgensen, K., and Norden, B., 2009. Application of the continuous wavelet transform on seismic data for mapping of channel deposits and gas detection at the CO2SINK site, Ketzin, Germany. Geophysical Prospecting. 57, 111-123.

Krumhans, J., Pawar, R., Grigg, R., Westrich, H., Warpinski, N., Zhang, D., Jove-Colon, C., Lichtner, P., Lorenz, J., Svec, R., Stubbs, B., Cooper, S., Bradley, C., Rutledge, J., and Byrer, C., 2002. Geological sequestration of carbon dioxide in a depleted oil reservoir. SPE/DOE Improved Oil Recovery Symposium

Litynski, J.T., Plasynski, S., McIlvried, H.G., Mahoney, C., and Srivastava, R.D., 2008. The United States Department of Energy's regional carbon sequestration partnerships program validation phase. Environment International. 34, 127-138.

Lozano, F.A. and Marfurt, K.J., 2008. 3D seismic visualization of shelf-margin to slope channels using curvature attributes. 78th Annual International Meeting, Society of Exploration Geophysicists. Technical Program Expanded Abstracts, 914-918.

Marfurt, K.J., Scheet, R.M., Sharp, J.A., and Harper, M.G., 1998. Suppression of the acquisition footprint for seismic sequence attribute mapping. Geophysics. 63, 1024-1035.

Mathieson, A., Wright, I., Roberts, D., and Ringrose, P., 2009. Satellite imaging to monitor CO2 movement at Krechba, Algeria. Energy Procedia. 1, 2201-2209.

Merriam, D.F., 1963. The geologic history of Kansas. Kansas Geological Survey. Bulletin 162, 135-151.

Prensky, S.E., 1997. Salina Basin province and Sedgwick Basin province. Kansas Geological Survey, Digital Petroleum Atlas. http://www.kgs.ku.edu/DPA/NMC/Prov/sedgwick.html.

Raef, A.E. and Slusarczyk, R., 2001. Factor analysis of seismic multiattributes for predicting porosities using sequential nonlinear regression: the thin carbonates of the BMB Field, Poland. Petroleum Geoscience. 7, 359-369.

Raef, A.E., Miller, R.D., Franseen, E.K., Byrnes, A.P., Watney, W.L., and Harrison, W.E., 2005. 4D seismic to image a thin carbonate reservoir during a miscible CO2 flood: Hall-Gurney Field, Kansas, USA. The Leading Edge. 24, 521-526.

Reynolds, J.M., 1997. An introduction to applied and environmental geophysics. John Wiley & Sons, England.

Russell, B.H., Hampson, D.P., and Lines, L.R., 2003. Application of the radial basis function neural network to the prediction of log properties from seismic attributes—A channel sand case study. SEG Technical Program Expanded Abstracts. 22. 454-457.

Saggaf, M.M., Toksoz, M.N., and Marhoon, M.I., 2003. Seismic facies classification and identification by competitive neural networks. Geophysics. 68. 6. 1984-1999.

Suarez, Y., Marfurt, K.J., and Falk, M., 2008. Seismic attribute-assisted interpretation of channel geometries and infill lithology: A case study of Anadarko Basin Red Fork channels. 78th Annual International Meeting, Society of Exploration Geophysicists. Annual Meeting, 963-967.

Sundquist, E., Burruss, R., Faulkner, S., Gleason, R., Harden, J., Kharaka, Y., Tieszen, L., and Waldrop, M., 2008. Carbon sequestration to mitigate climate change. U.S. Geological Survey. Fact Sheet 2008-3097.

Torp, T.A. and Gale, J. 2004. Demonstrating storage of CO2 in geological reservoirs: The Sleipner and SACS projects. Energy. 29, 1361-1369.

West, B.P., May, S.R., Eastwood, J.E., and Rossen, C., 2002. Interactive seismic facies classification using textural attributes and neural networks. The Leading Edge. 21. 10. 1042-1049.

Zeller, D.E., 1968. The stratigraphic succession in Kansas. Kansas Geological Survey. Bulletin 189, 7-23.

Ziolkowski, A., Underhill, J.R., and Johnston, R.G.K., 1998. Wavelets, well ties, and the search for subtle stratigraphic traps. Geophysics. 63. 297-313.